

NUREG/CR-4681
SAND86-1296
RP
Printed March 1987

Enclosure Environment Characterization Testing for the Base Line Validation of Computer Fire Simulation Codes

S. P. Nowlen

Prepared by
Sandia National Laboratories
Albuquerque, New Mexico 87185 and Livermore, California 94550
for the United States Department of Energy
under Contract DE-AC04-76DP00789

Prepared for
U. S. NUCLEAR REGULATORY COMMISSION

SF2900Q(8-81)



NOTICE

This report was prepared as an account of work sponsored by an agency of the United States Government. Neither the United States Government nor any agency thereof, or any of their employees, makes any warranty, expressed or implied, or assumes any legal liability or responsibility for any third party's use, or the results of such use, of any information, apparatus product or process disclosed in this report, or represents that its use by such third party would not infringe privately owned rights.

Available from
Superintendent of Documents
U.S. Government Printing Office
Post Office Box 37082
Washington, D.C. 20013-7082
and
National Technical Information Service
Springfield, VA 22161

NUREG/CR-4681
SAND86-1296
RP

**ENCLOSURE ENVIRONMENT CHARACTERIZATION TESTING FOR THE
BASE LINE VALIDATION OF COMPUTER FIRE SIMULATION CODES**

S. P. Nowlen

March 1987

**Sandia National Laboratories
Albuquerque, NM, 87185
Operated by
Sandia Corporation
for the
U.S. Department of Energy**

**Prepared for
Electrical Engineering Branch
Office of Nuclear Regulatory Research
U. S. Nuclear Regulatory Commission
Washington, DC 20555
Under Memorandum of Understanding DOE 40-550-75
NRC FIN No. A1010**

Abstract

This report describes a series of fire tests conducted under the direction of Sandia National Laboratories for the U. S. Nuclear Regulatory Commission. The primary purpose of these tests was to provide data against which to validate computer fire environment simulation models to be used in the analysis of nuclear power plant enclosure fire situations. Examples of the data gathered during three of the tests are presented, though the primary objective of this report is to provide a timely description of the test effort itself.

These tests were conducted in an enclosure measuring 60x40x20 feet constructed at the Factory Mutual Research Corporation fire test facility in Rhode Island. All of the tests utilized forced ventilation conditions. The ventilation system was designed to simulate typical nuclear power plant installation practices and ventilation rates.

A total of 22 tests using simple gas burner, heptane pool, methanol pool, and PMMA solid fires was conducted. Four of these tests were conducted with a full-scale control room mockup in place. Parameters varied during testing were fire intensity, enclosure ventilation rate, and fire location.

Data gathered included air temperatures, air velocities, radiative and convective heat flux levels, optical smoke densities, inner and outer enclosure surface temperatures, enclosure surface heat flux levels, and gas concentrations within the enclosure in the exhaust stream.

Suggested key words:

- Fire Modeling
- Fire Testing
- Enclosure Fires
- Base Line Validation Testing
- Nuclear Power Plants

Table of Contents

| | <u>Page</u> |
|--|-------------|
| Executive Summary | 1 |
| 1.0 Introduction | 3 |
| 2.0 The Test Enclosure | 5 |
| 3.0 Enclosure Instrumentation | 7 |
| 4.0 Test Parameters and the Test Matrix | 13 |
| 4.1 Fuel/Fire Source Parameters | 13 |
| 4.2 Fire Locations | 16 |
| 4.3 Enclosure Ventilation Rate | 16 |
| 4.4 Room Configuration | 17 |
| 4.5 The Test Matrix | 17 |
| 5.0 Examples of Available Data | 17 |
| 6.0 Conclusions | 39 |
| References | 42 |
| Appendix A: Test Facility Construction Details | |
| Appendix B: Test Instrumentation Details | |
| Appendix C: Calculation of Heat Release Rates | |

List of Figures

| | <u>Page</u> |
|--|-------------|
| Figure 1: Enclosure Ventilation System. | 6 |
| Figure 2: Placement of Instrument Trees Within the Test Enclosure. | 11 |
| Figure 3: Definition of Instrumentation on Each of the Instrument Trees Types Shown in Figure 1. | 12 |
| Figure 4: Heat Release Rate Profiles Followed for the Gas Burner Tests Using the Growth Mode. | 15 |
| Figure 5: Control Room Mockup Configuration of the Test Enclosure. | 18 |
| Figure 6: Heat Release Rates Calculated Based on Generation Rate of Carbon Dioxide for Tests 4, 5, and 21. | 20 |
| Figure 7: Three-Dimensional Plot of Temperature Versus Plan View Location for the 6-Foot Elevation at 5 and 10 Minutes After Ignition in Test 5. | 22 |
| Figure 8: Three-Dimensional Plot of Temperature Versus Plan View Location for the 10-Foot Elevation at 5 and 10 Minutes After Ignition in Test 5. | 23 |
| Figure 9: Three-Dimensional Plot of Temperature Versus Plan View Location for the 14-Foot Elevation at 5 and 10 Minutes After Ignition in Test 5. | 24 |
| Figure 10: Three-Dimensional Plot of Temperature Versus Plan View Location for the 18-Foot Elevation at 5 and 10 Minutes After Ignition in Test 5. | 25 |
| Figure 11: Three-Dimensional Plot of Temperature Versus Plan View Location for the 19-Foot, 7-Inch Elevation at 5 and 10 Minutes After Ignition in Test 5. | 26 |
| Figure 12: Smoke Optical Density to Blue Light at Each of Two Elevations on Sector 2 Instrument Tree During Tests 4, 5, and 21. | 27 |
| Figure 13: Vertical Temperature Profile at Sector 2 Location During Fire Growth and Fire Steady-State Periods of Tests 4, 5, and 21. | 28 |

| | |
|---|-----------|
| Figure 14: Vertical Temperature Profiles at Sector 2 Location Following Fire Extinguishment In Tests 4, 5, and 21. | 29 |
| Figure 15: Data From Bare-Bead and Aspirated Thermocouples at Sector 2, 6-Foot Location During Test 4. | 32 |
| Figure 16: Data From Bare-Bead and Aspirated Thermocouples at Sector 2, 6-Foot Location During Test 5. | 33 |
| Figure 17: Data From Bare-Bead and Aspirated Thermocouples at Sector 2, 6-Foot Location During Test 21. | 34 |
| Figure 18: Raw Data and Curve Fit for Sector 2, 6-Foot Location Sphere Calorimeter Processing During Test 5. | 36 |
| Figure 19: Equivalent Radiative Environment Temperature Derived Based on Sphere Calorimeters at Sector 2, 6 Foot Location During Test 5. | 37 |
| Figure 20: Net Heat Flux Levels for Sphere Calorimeters at Sector 2, 6 Foot Location During Test 5. | 38 |
| Figure 21: Carbon Dioxide and Carbon Monoxide Concentrations at Sector 2 During Test 5. | 40 |

List of Tables

| | <u>Page</u> |
|---|-------------|
| Table 1: Matrix of Base Line Validation Tests Conducted in the Open Enclosure Configuration | 8 |
| Table 2: Matrix of Base Line Validation Tests Conducted in the Control Room Mockup Configuration | 9 |

Acknowledgements

The author thanks the Factory Mutual Research Corporation staff who were responsible for the conduct of these tests. In particular Jeff Newman and John Hill have earned our thanks. Their experience was invaluable to the execution of this ambitious effort.



Executive Summary

This report describes a series of fire tests conducted under the direction of the Adverse Environment Safety Assessment Division (6447) of Sandia National Laboratories for the U. S. Nuclear Regulatory Commission. The primary purpose of these tests was to provide data on various characteristics of the environment within a nuclear power plant sized enclosure during a fire. It is intended that this data be used for the base line validation of computer fire environment simulation models. A secondary purpose of these tests was to act as facility shakedown and calibration tests prior to execution of a series of electrical cabinet fire tests within the test enclosure. The electrical cabinet fire tests are described in a separate work.[7]

These tests were conducted by the Factory Mutual Research Corporation under direct contract to Sandia. The tests were conducted in an enclosure built by Factory Mutual within a larger fire test structure in Rhode Island. The test enclosure itself measured 60 feet long, by 40 feet wide, by 20 feet tall (approximately 18x12x6 meters). Forced ventilation conditions were used in all of the tests. Ventilation was supplied through a system installed in the enclosure that simulated typical nuclear power plant ventilation installation practices and ventilation rates.

An extensive array of instrumentation was installed in order to monitor a variety of aspects of the environment within the enclosure. For characterization of the enclosure air a total of 92 thermocouples, 18 sphere calorimeters (for the measurement of convective and radiative heat fluxes), 6 smoke optical density meters, 9 three-dimensional velocity probes, and 9 gas concentration sampling ports was utilized. The walls, ceiling, and floor of the enclosure were instrumented for combinations of inner surface temperature and inner surface heat flux, and in the case of the walls and ceiling, outer surface temperature. The exhaust gas duct was monitored for concentrations of oxygen, carbon monoxide, carbon dioxide, and unburned hydrocarbons. For each test a total of over 300 channels of data was generated.

Twenty-two tests, using simple well-defined propylene gas, heptane pool, methanol pool, and polymethyl methacrylate (PMMA) solid source fuel fires, were conducted. Other parameters varied during testing were fire location, fire intensity, enclosure ventilation rate, and room configuration. Room configuration was varied in that 4 of these 22 tests were conducted in a control room mockup configuration of the test enclosure.

The primary goal of this report is to provide a timely description of the test effort. A secondary goal is to provide examples of the data available as a result of the effort. Examples are presented from three similar tests (Tests 4, 5, and 21). Four conclusions are drawn based on this limited data presentation:

1. Thermal radiation plays a significant role in the heating of the enclosure air for test fires conducted in an open, unshielded location.
2. Hot layer temperatures during these tests were quite low compared to previous enclosure fire test efforts presumably due to the large size of the test enclosure and the ventilation conditions used in the present effort.
3. The configuration of the ventilation system resulted in the partitioning of the hot layer into two distinctly different layers.
4. Even an air exchange rate of 10 room air changes per hour was not sufficient to prevent the buildup of a dense smoke layer within the enclosure that descended to floor level within ten minutes of fire ignition during every test other than those involving the clean burning methanol and PMMA fuel fires.

1.0 INTRODUCTION

The primary objective of the Base Line Validation Test Program is to provide benchmarking test results for use in the development and validation of computer fire codes to be used for predicting fire-induced environments in nuclear power plant enclosures. The Base Line Validation Tests described here were designed to provide test data characterizing a number of aspects of the room environment from an extensively instrumented enclosure under a variety of fairly simple, well-defined fire conditions. This data may be used to validate a variety of fire codes, including so-called zone models and field models.

A secondary purpose of the tests described here was to act as facility shakedown and calibration tests prior to the execution of a series of electrical control cabinet fire tests in the same test enclosure. These cabinet fire tests, described in a separate work [7], involved the burning of complex cable configurations within a control room mockup in the test enclosure. Because of the extent of instrumentation utilized in these tests, it was desirable to perform the simpler tests described here prior to the conduct of the more complicated cabinet tests. This allowed personnel to work out minor "bugs" in the instrumentation, facility, and test procedures during relatively inexpensive and easily repeated tests. The data from the simple fuel tests also allows for calibration and verification of the heat release rate calculation procedure, which will be of primary interest in analysis of the cabinet fire test data. This calculation process is described in Appendix C.

The tests described here were conducted by Factory Mutual Research Corporation (FMRC) under the direction of Sandia National Laboratories (SNL) in an enclosure at the FMRC test site in Rhode Island. This enclosure was intended to be representative of a credible nuclear power plant enclosure. The enclosure has dimensions of 60 feet long, by 40 feet wide, by 20 feet high (18x12x6 meters). Forced ventilation conditions were used in all of the tests described here. Section 2 of this report provides more detail on the characteristics of the test enclosure. Appendix A provides details on the actual construction of the test enclosure as provided by FMRC.

The enclosure was instrumented with a variety of instrumentation including an extensive array of thermocouples, heat flux probes, one-, two-, and three-dimensional velocity probes, smoke density meters, and gas sampling ports for the analysis of oxygen, carbon dioxide, carbon monoxide, and unburned pyrolytate concentrations. Section 3 provides more detail on the distribution of instrumentation within the

test enclosure, on the surfaces of the test enclosure, and in the inlet and exhaust ducts. Appendix B gives additional information on the type of instrumentation used, the data logging system used, and the actual channel maps for data collected. The information in Appendix B was provided by FMRC.

The test fires utilized in the Base Line Validation Tests involved a variety of simple, well-defined gas burner, liquid pool, and solid fuel fires (the fire sources are described in detail in Section 4.1). The tests explored the effects of fuel type, fire intensity, fire placement, ventilation rate, and room configuration on the development of the room environment. A total of 22 tests utilizing these simple, well-defined fire sources was conducted. Of these tests, 18 were conducted in the enclosure with no internal partitioning. The remaining 4 tests were conducted with a full-scale control room mockup in the test enclosure.

The results of these tests should be useful in validating the computer fire codes traditionally used in nuclear power plant fire risk analyses. Detailed enclosure fire test data for enclosures such as those found in a nuclear power plant were not available previously. This lack of adequate test data has resulted in the use of fire codes in situations for which they were not originally intended and for which they have never been validated. The particular areas of concern typically voiced involve the enclosure size (most test results available involve use of residential or single office sized enclosures), the density of test enclosure instrumentation (typical tests involve instrumentation for a very few specific aspects of fire development rather than a general array encompassing a variety of instrumentation), and the ventilation conditions utilized (most codes and tests deal primarily with the naturally ventilated fire, whereas most nuclear power plant enclosures are exclusively forced ventilated).

The instrumentation plan was developed with input from those at Brookhaven National Laboratories (BNL), the CHAM group of Atlanta, and the U.S. Nuclear Regulatory Commission (NRC). The instrumentation density was considered adequate for validating even three-dimensional thermal hydraulic finite difference flow codes (i.e., field models). The field modeling approach is one in which the enclosure of interest is represented by a large number of nodal computation points (on the order of 100-1000 nodes). The major characteristics of concern (temperature, pressure, gas concentrations, etc.) are then calculated for each node with the solution at each node iterated forward in time for the entire enclosure. Such extensive detail in the calculation process called for a similar level of detail in the instrumentation package for

the test enclosure. The enclosure instrumentation was designed to provide information on variations of environmental conditions in both the horizontal and vertical directions.

Other fire codes, including those that utilize a zone modeling approach, should also benefit from this data. Under the zone modeling approach, the enclosure of interest is typically divided into two or three lumped zones; a hot upper layer, a cool lower layer, and in some cases the fire plume. Transfer of mass and energy between these lumped zones is tracked mathematically. Thus the zone models generate less specific detail on environmental conditions. This lack of detail is somewhat compensated through simplicity of calculation procedures and reduced calculation times.

2.0 THE TEST ENCLOSURE

The enclosure used for the tests described here is located at the FMRC test site in Rhode Island. The entire test enclosure is itself housed within an outer building and hence isolated from the external environment. The basic structure of the test enclosure was used in previous cable tray fire tests conducted by FMRC. For the purposes of this test program, the enclosure was expanded to a size of 60 feet long by 40 feet wide by 20 feet high (18x12x6 meters). The inside surfaces of the enclosure ceiling and walls were lined with one-inch thick marinite panels in an effort to simulate the behavior and characteristics of concrete walls such as those encountered in nuclear power plants. These one-inch marinite panels were expected to behave much like a concrete wall for the duration of the tests anticipated. Analysis of wall temperature data obtained during testing should define the validity of this assumption though this analysis has not yet been performed. The floor of the enclosure was comprised of the concrete slab making up the foundation of the test building.

A forced ventilation system with six inlet ports (one inlet per 400 square feet (37 square meters) of floor area) and one outlet port were installed in the enclosure as shown in Figure 1. This system was capable of providing ventilation rates equivalent to from one to ten room air changes per hour. The inlet ports extended down through the ceiling of the enclosure to a point four feet (1.2 m) below the ceiling, with air directed downward out of the inlets. These inlets were capped with standard, commercially available four-way air diffusers. The inlet ports were extended in this way in order to simulate typical design practices in nuclear power

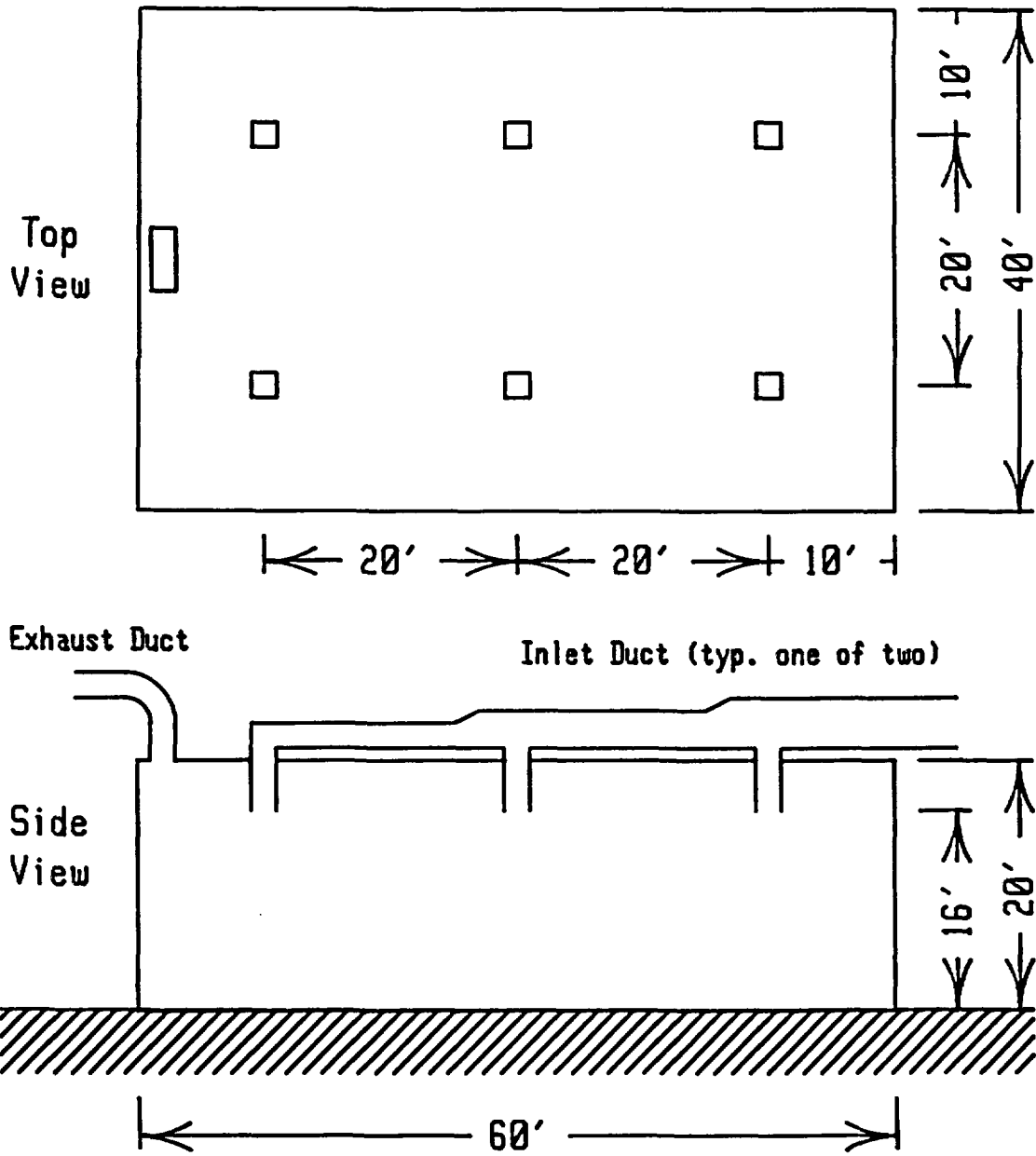


Figure 1: Enclosure ventilation system.

plants while at the same time introducing as few internal obstructions within the enclosure as possible. Typical power plant installations involve an air duct run at some distance (3-5 feet) below the true ceiling with ventilation grills set into the bottom of this air duct. Simulation of the height at which the inlet air was introduced into the enclosure and the available ventilation flow rate were considered the primary effects of interest.

A single outlet port was located in the ceiling along the east wall of the test enclosure (one of the short walls). The outlet was placed in the ceiling in order to increase the sensitivity of the exhaust duct instrumentation to changes in the fire intensity. The outlet duct was sized such that the minimum pressure drop through the outlet for anticipated ventilation rates would be 1/8 inch of water. This pressure corresponds to typical control room operating pressures. Totally unrestricted air flow out of the enclosure would not be representative of actual power plant conditions.

The first 18 Base Line Validation Tests were conducted in the enclosure with no internal obstructions present. The conditions used in each of these tests are shown in Table 1. The remaining four Base Line Validation Tests were conducted in a control room mockup configuration of the test enclosure. The test conditions for each of these four tests are shown in Table 2.

The control room mockup included six "real" electrical control cabinets (three benchboard style, one mitered corner benchboard style, and two single-bay vertical style). The remainder of the mockup was constructed from marinite panels bolted to metal framing material. The height of the entire mockup was 8 feet. The actual dimensions of each of the sections of the control room mockup are described in Section 4.4.

Appendix A provides a complete description of the test enclosure, including construction details, prepared by the contractor, FMRC.

3.0 ENCLOSURE INSTRUMENTATION

This section contains a description of the general enclosure instrumentation utilized during the Base Line Validation Tests. Appendix B, provided by FMRC, gives additional detail on the data logging system and on the types of instrumentation used.

Table 1: Matrix of Base Line Validation Tests conducted in the open enclosure configuration.

| | | Test # | 1 | 2 | 3 | 4 | 5 | 6 | 7 | 8 | 9 | 10 | 11 | 12 | 13 | 14 | 15 | 16 | 17 | 18 |
|------------------------------------|----------------------|--------|---|---|---|---|---|---|---|---|---|----|----|----|----|----|----|----|----|----|
| Fuel Type | Propylene Burners | X | X | X | X | X | | X | X | X | | | | | | | | | | |
| | Heptane Pool | | | | | | X | | | | X | | X | X | | X | X | X | | |
| | Methanol Pool | | | | | | | | | | | X | | | X | | | | | |
| | PMMA Solid Slabs | | | | | | | | | | | | | | | | | | | X |
| Nominal Peak Fire Intensity | 500 kW | X | X | | X | X | X | X | | | | X | | | X | | X | X | | |
| | 1000 kW | | | | | | | | | X | X | X | | | | X | | | | X |
| | 2000 kW | | | X | | | | | | | | | X | X | | | | | | |
| Fire Location | Room Center | X | X | X | X | X | | X | X | X | | | | | | | | | | |
| | South Wall | | | | | | X | | | | X | X | X | X | X | X | | | | X |
| | S-W Corner | | | | | | | | | | | | | | | | X | X | | |
| Nominal Enclosure Ventilation Rate | 1 ch/hr (800 CFM) | | | | X | | X | X | X | | | | | | X | X | X | | | X |
| | 4.4 ch/hr (3500 CFM) | | | | | | | | | | X | X | X | | | | | | | |
| | 8 ch/hr (6400 CFM) | | | | | | | | | X | | | | X | | | | | | |
| | 10 ch/hr (8000 CFM) | X | X | X | | X | | | | | | | | | | | | | | X |
| Burner Fire Mode | Steady State Mode | X | X | X | | | | | | X | | | | | | | | | | |
| | Growing Fire Mode | | | | X | X | | | | | X | X | | | | | | | | |

Table 2: Matrix of Base Line Validation Tests conducted in the control room mock up configuration.

| | | Test # | | | |
|------------------------------------|------------------------|--------|----|----|----|
| | | 19 | 20 | 21 | 22 |
| Fuel Type | Propylene Burner | | | X | X |
| | Heptane Pool | X | X | | |
| Nominal Peak Fire Intensity | 500 kW | | | X | |
| | 1000 kW | X | X | | X |
| Fire Location | Room Center | X | | | |
| | South-West Corner | | X | | |
| | Benchboard Cabinet 'A' | | | X | X |
| Nominal Enclosure Ventilation Rate | 1 ch/hr (800 CFM) | X | | X | X |
| | 8 ch/hr (6400 CFM) | | X | | |
| Gas Burner Fire Mode | Steady State Mode | | | | |
| | Growing Fire Mode | | | X | X |

Figures 2 and 3 illustrate the placement of most of the general enclosure instrumentation. Figure 2 shows the placement of the instrument trees, which have been grouped into four types: stations, expanded stations, corner rakes, and sectors within the enclosure. Figure 3 defines the instrumentation included on each of these four general types of instrumentation trees. As can be seen from Figure 3, the sectors represent the most heavily instrumented locations and the stations the most lightly instrumented locations.

The sum of the instrumentation represented by these 21 instrument trees provided the following instrumentation for characterization of the environment associated with the air in the enclosure:

- 31 aspirated thermocouples
- 59 bare-bead thermocouples
- 9 small sphere calorimeters
- 9 large sphere calorimeters
- 6 smoke turbidimeters (smoke density meters)
- 9 three-dimensional velocity probes
- 9 gas sampling ports (for oxygen, carbon dioxide, carbon monoxide)

The large and small sphere calorimeters were located in pairs in nine locations within the room. Together with the gas temperature measurements provided by the aspirated thermocouples these calorimeters can provide estimates of both the convective and radiative heat transfer rates to the spheres. The convective heat transfer rates can also be converted to bulk flow velocity information through correlations that relate the heat transfer coefficient to the velocity of the air flow. This calculation procedure has been described by Newman [1].

The optical smoke density meters, or smoke turbidimeters, are devices designed by FMRC for use in fire testing. Of the six devices installed in the enclosure, five utilized a single color light extinction measurement. The final turbidimeter utilized a three-wavelength light extinction measurement. Through experimental use FMRC has shown a correlation between the optical density of the smoke at a particular wavelength to the volume fraction of smoke. Thus these optical extinction measurements can be used to estimate the smoke volume fraction in the area of measurement. Data from the three-wavelength device can also be used to generate estimates of the particulate sizes in the area of the device. The details of construction and use of the turbidimeters have been described by Newman [2]. The procedures for processing the turbidimeter data have also been described by Newman in a separate work [3].

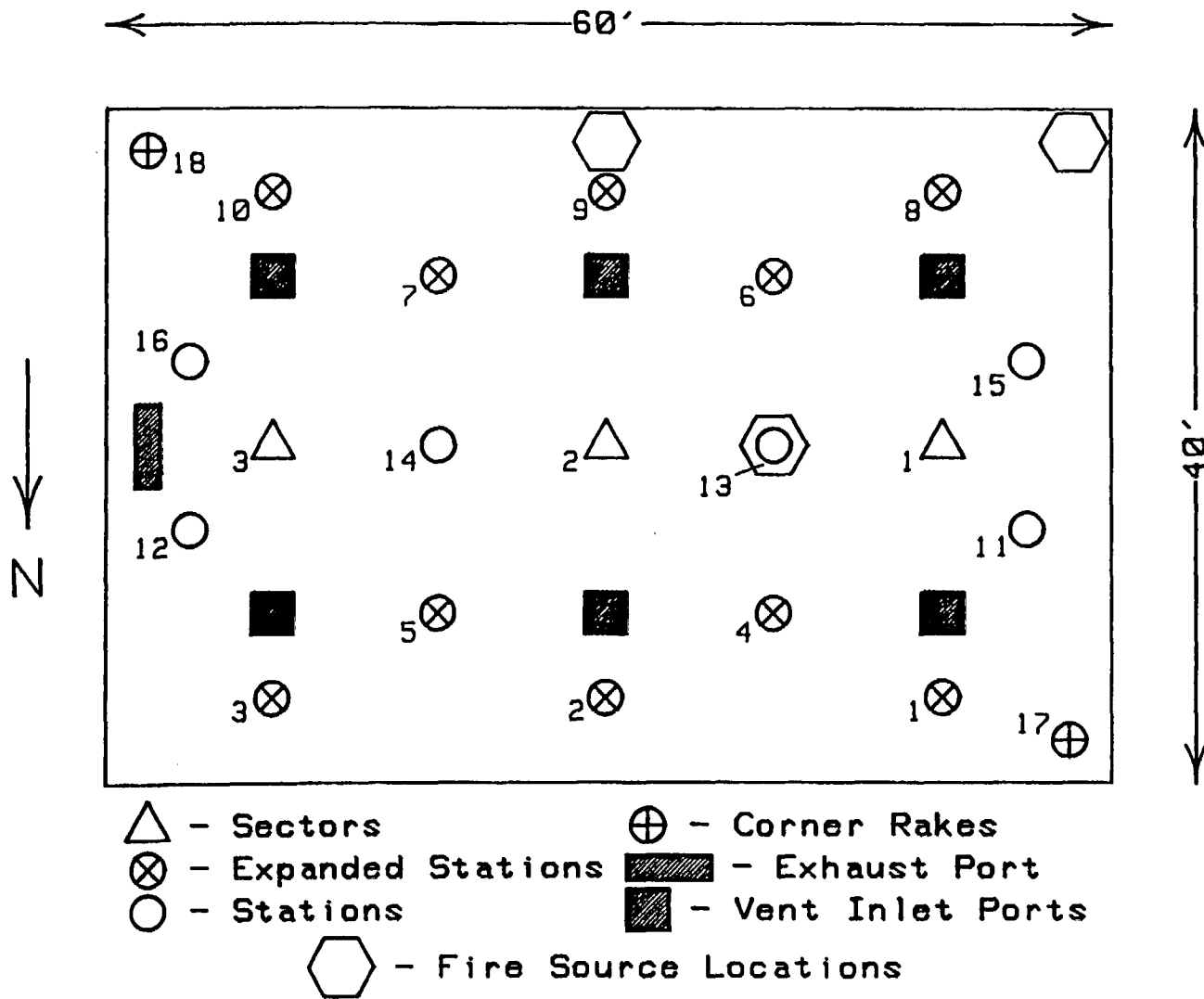


Figure 2: Placement of instrument trees within the test enclosure.

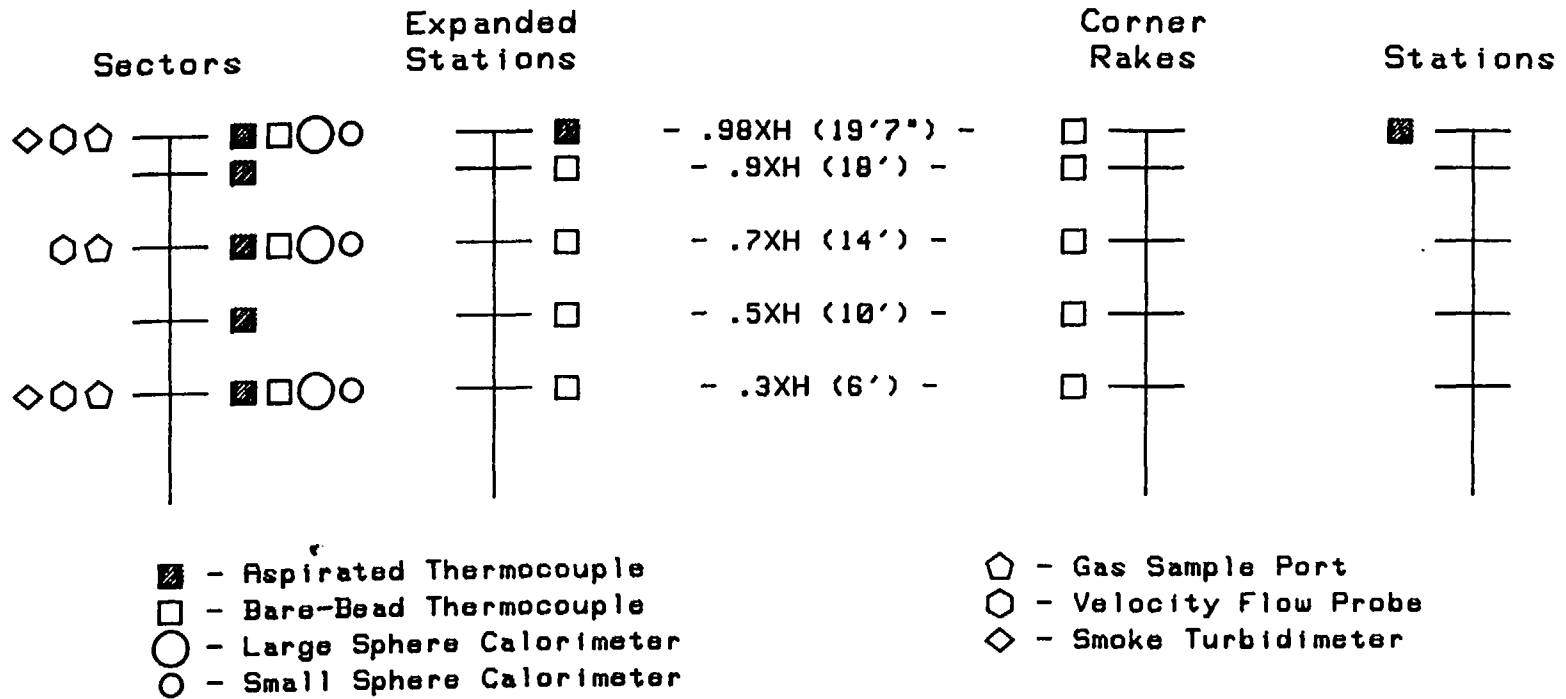


Figure 3: Definition of instrumentation on each of the instrument tree types shown in Figure 2.

The enclosure surfaces were instrumented at a number of locations for surface temperature and surface heat flux. The ceiling was instrumented at four locations for inner surface temperature only, at six additional locations for both inner surface heat flux and inner surface temperature, and at three additional locations for inner surface heat flux and both inner and outer surface temperature. These locations are described in Appendix B. Similarly, the enclosure walls were instrumented at twelve locations for inner surface temperature only, and at an additional eight locations for inner surface heat flux and both inner and outer surface temperature. These locations are described in Appendix B. The floor of the enclosure was instrumented at three locations for upper surface heat flux and temperature. These three locations correspond to the locations of the three instrumentation sectors shown in Figure 2.

Differential pressure measurements were made in both the main inlet ventilation duct and the outlet ventilation duct for calculation of duct velocity. The static pressure in the chamber was also monitored at two locations.

Fuel burning rates for the liquid fuel pool fires and the solid fuel fire were monitored using a load platform to measure the fuel mass remaining throughout each test.

Concentrations of oxygen, carbon dioxide, carbon monoxide, and unburned hydrocarbons were continuously measured in the exhaust duct.

In all, over 300 channels of data were generated during each of the fire tests. Data on the convective and radiative heat flux levels in the room, temperatures in the enclosure and on the inner and outer surfaces of the enclosure, smoke densities, and gas concentrations both within the enclosure and in the exhaust gas is available. Channel maps for the data files generated in each test are presented in Appendix B.

4.0 TEST PARAMETERS AND THE TEST MATRIX

4.1 Fuel/Fire Source Parameters

The fuel/fire sources utilized in the tests described here fall into three basic categories:

1. gas burner fires,
2. liquid pool fires,
3. simple solid fuel fires.

Each of these basic categories of fire and the nominal fire intensities used within each of these categories is discussed below.

Ten tests utilizing a gas burner were conducted (see the test matrix presented in Tables 1 and 2). Two of these ten tests were conducted in the control room mockup configuration of the test enclosure with the burner placed inside one of the benchboard cabinets. The burner utilized was a 36-inch diameter sand burner. The gaseous fuel was forced to flow up through a base of loose sand filling the burner body. As the gas was not premixed with air, a diffusion flame resulted. The base of this flame was approximately 12 inches above the floor of the enclosure. In all cases the gas utilized was propylene.

These ten gas burner tests each used one of three nominal peak values of the heat release rate: 516, 1000, and 2000 kW. The gas test fires were conducted in both a steady state and in a growing fire mode as indicated in the test matrix (see Tables 1 and 2). For the steady-state tests the burners were activated at the indicated peak rate and allowed to burn for approximately 10 minutes. In the growth-mode tests the burners were made to provide an increasing flow rate from zero flow to the indicated peak rate at a pre-programmed rate. The flow rate was made proportional to the square of elapsed time from ignition to full intensity. The peak value was maintained for a prescribed period to provide a total burn duration of 10 minutes for the 516 kW fires and 13 minutes for the 1000 kW fires. Following this hold at peak intensity, the burners were shut off. The profiles used for the two peak fire intensities used for growth-mode tests are shown in Figure 4.

For the two control room mockup tests using the gas burner, one test utilized a peak heat release rate of 516 kW, while the other used a peak heat release rate of 1000 kW. Both tests utilized a growth-mode fire such as those described above. The only exception to the discussion above was that the fires were allowed to burn for a total of approximately 19 and 14 minutes respectively.

Nine tests involving various flammable liquid fuel pool fires were conducted. These pool fires utilized three nominal heat release rates: 500, 1000, and 2000 kW. These heat release rates correspond to those used in the gas burner tests. Two liquid fuels were used: methanol and heptane. These two fuels were chosen as representative of "clean" and "dirty" burning fuels, respectively.

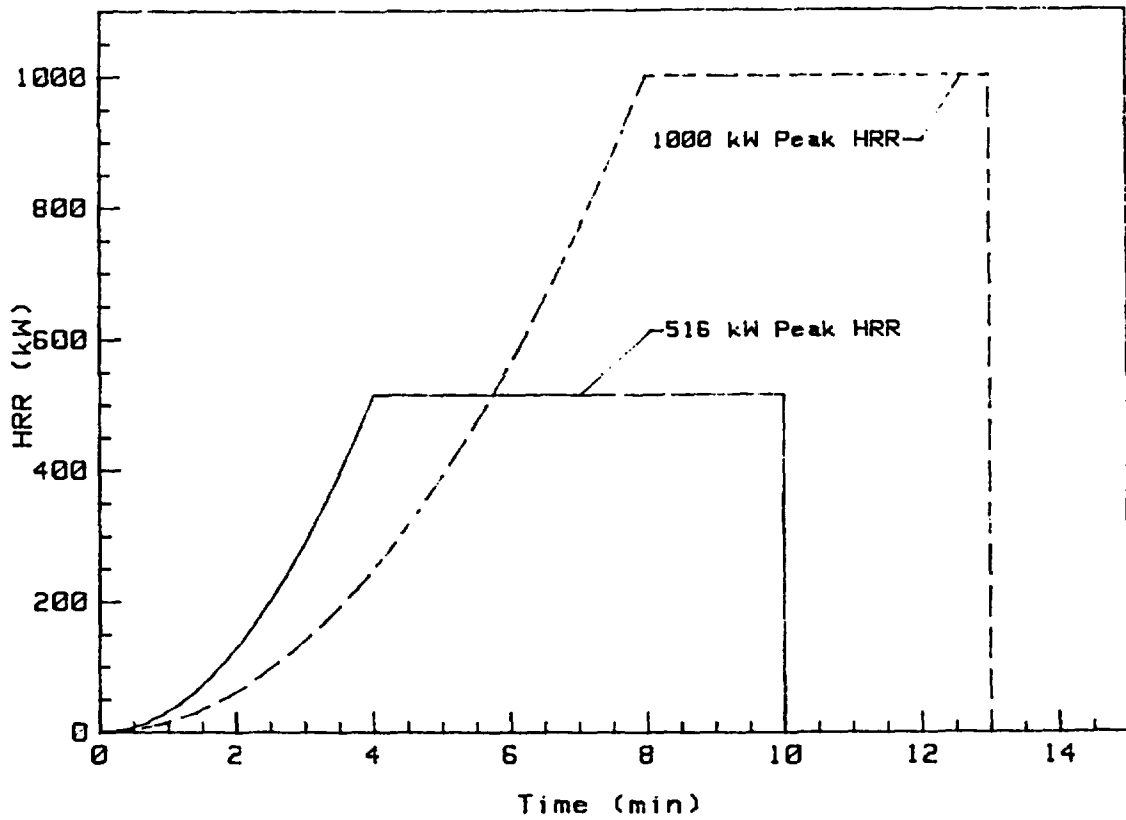


Figure 4: Heat Release Rate Profiles Followed for the Gas Burner Tests Using the Growth Mode.

One test was conducted using a simple configuration of two works polymethyl methacrylate (PMMA) as the fuel source. This fuel source utilized two 2'x2'x1" (0.6m x 0.6m x 2.5cm) slabs of PMMA in a nearly vertical orientation with a small pan of methanol placed between them as an ignition source. This fire was estimated to have a peak heat release rate of 1000 kW. This fuel source was chosen to represent an uncontrolled solid fuel fire. PMMA was selected as the material to be utilized as it has been extensively used in many studies and is hence one of the best characterized of the plastic materials available. The configuration was purposely kept as simple as possible in order to make post-test data interpretation as simple as possible.

4.2 Fire Locations

For the tests conducted in the open enclosure, fires were placed in three locations: near the center of the room, along the center of the south wall, and in the southwest corner. Figure 2 shows each of these locations. These three locations were selected as locations that should yield somewhat different room environments for a given fire. This should present differing challenges to field computer fire codes, testing their ability to accurately simulate subtle changes in the nature of the enclosure fire. It is a field code's potential for sensing such subtle differences that sets it apart from the simpler zone computer fire codes.

For the tests conducted in the control room mockup, fires were placed in three locations. For the two tests involving gas burners, the burner was located inside of benchboard cabinet "A" as shown in Figure 5. For the two heptane pool fires, the room center and south wall locations as described above were used.

4.3 Enclosure Ventilation Rate

Four nominal ventilation rates were used: 1 room change per hour, 4.4 room air changes per hour, 8 room air changes per hour, and 10 room changes per hour. These rates correspond to 800 CFM (0.38 m³/s), 3500 CFM (1.65 m³/s), 6400 CFM (3.02 m³/s), and 8000 CFM (3.78 m³/s) respectively. The lowest ventilation rate corresponds to typical ventilation rates for general nuclear power plant enclosures and some control rooms. The highest rate corresponds to that suggested by a proposed guideline for control room smoke purging capability from the Control Room Habitability Working Group issued in June 1984. The middle two rates correspond to typical ventilation rates under normal conditions for many nuclear power plant control rooms, with 8 room air exchanges per hour being on the high side of normal.

4.4 Room Configurations

The room configuration parameter refers to the fact that four of the Base Line Validation Tests, 19-22, were conducted in the control room mockup configuration of the test enclosure. A schematic of the control room mockup including dimensions is presented in Figure 5. These control room mockup tests should be helpful in characterizing the degree to which the presence of a large number of cabinets, which play the role of internal partitions, affect the development of the room environment.

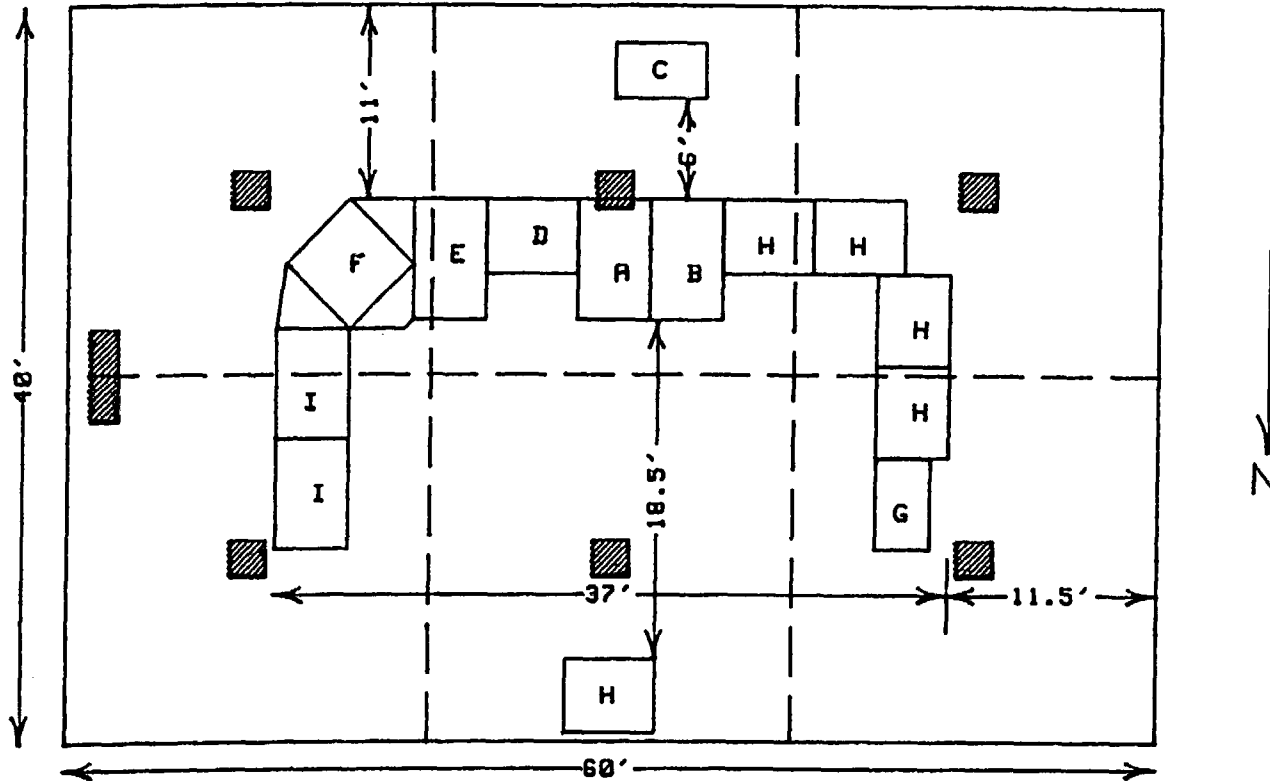
4.5 The Test Matrix

The matrix of tests performed under the Base Line Validation Test Program is presented in Tables 1 and 2. A total of 22 tests was performed using the simple fuel sources described above. Of these 22 tests, 18 were performed in the open test enclosure. These 18 open enclosure tests are described in Table 1. The remaining 4 tests were conducted in the control room mockup configuration of the test enclosure. Table 2 describes the 4 control room mockup tests conducted using these simple fuels.

5.0 EXAMPLES OF AVAILABLE DATA

It is not the purpose of this report to provide an exhaustive treatment of the test data. Nor is it intended that the treatment here include full interpretation of the results presented. The purpose of this report is to provide the reader with a timely description of the test effort and of the type of data that can be made available. The examples that follow represent only a small fraction of the data available for the tests discussed and for those tests still remaining. These examples were chosen because they illustrate some interesting and somewhat unexpected phenomena. These examples do raise fundamental questions regarding the development of a fire environment in large forced ventilated rooms. These questions cannot be fully resolved here. It is hoped that further analysis of the test data will help to answer these unresolved questions.

The results of Tests 4, 5, and 21 will be used to illustrate the type of data available as a result of these tests and some of the data presentation capabilities available. Each of these three tests involved a gas burner fire using a growth mode profile with a peak heat release rate of 516 kW. Tests 4 and 5 were conducted in the open configuration of the test enclosure with the burner in the room center location. Test 21 was conducted in the control room mockup configuration of the test enclosure with the fire placed inside benchboard cabinet "A" (see Figure 5). In Tests 4



CABINETS A,B,&E - BENCHBOARD CABINETS, 6.5X4X8 FT
CABINET F - MITERED BENCHBOARD CABINET, 6.5X6.5X8 FT
CABINETS C&G - VERTICAL CABINETS, 3X5X7.5 FT
CABINETS D&H - CABINET MOCKUPS, 4X5X8 FT
CABINETS I - CABINET MOCKUPS, 4X6X8 FT

Figure 5: Control room mockup configuration of the test enclosure.

and 21 a nominal ventilation rate of 1 room air change per hour was used. Test 5 utilized a nominal ventilation rate of 10 room air changes per hour. For these three tests the same source fire was burned in the open enclosure with both high and low ventilation rates and in both the open enclosure and control room mockup at the low ventilation rate. This allows for direct comparison of the test results.

Figure 6 shows the calculated heat release rates for each of these three tests as compared to the actual burner profile. These heat release rates are based on the generation rate of carbon dioxide. The calculation process, described in Appendix C, includes consideration of both the outflow gasses and the accumulation of carbon dioxide within the room. Because of the size of the test enclosure, the accumulation term accounts for a significant fraction of the total carbon dioxide generated. Note that the calculated values match the known profile quite well. In Test 5 a rapid spike in heat release rate is shown at 9 minutes. This spike corresponds to a test anomaly in which the ventilation blower overheated and shut down. This anomaly explains the behavior seen for Test 5 described in Appendix C.

One of the most vivid graphic data presentation techniques is illustrated in Figures 7 through 11. Referring to Figures 2 and 3 one will note that the instrumentation was concentrated on each of five vertically spaced horizontal planes within the enclosure. These planes were at elevations of 6 ft. (.3 x height (H)) (1.8 m), 10 ft. (.5 x H) (3.0 m), 14 ft. (.7 x H) (4.3 m), 18 ft. (.9 x H) (5.5 m), and 19 ft. 7 in. (.98 x H) (5.9 m). The plots shown in Figures 7 through 11 were generated using the thermocouple data from each of these five planes independently. For each plot the data at a given time for a given plane is used to generate a uniform grid of temperature versus plan view location (i.e., location as seen from directly above).

This uniform grid is generated through use of a distance weighting technique available in the commercial plotting routine DISSPLA [4]. This technique utilizes the available data from the nonuniform grid of instrumentation and a distance weighting factor (1.8 in the plots shown) to generate the uniform grid of data. At the location of an actual data point the true value is always used. Between the logged data points an interpolation is performed that weighs the available data within the search zone to the inverse of distance to the interpolation point raised to the weight factor power. The resulting grid was then plotted using other DISSPLA routines.

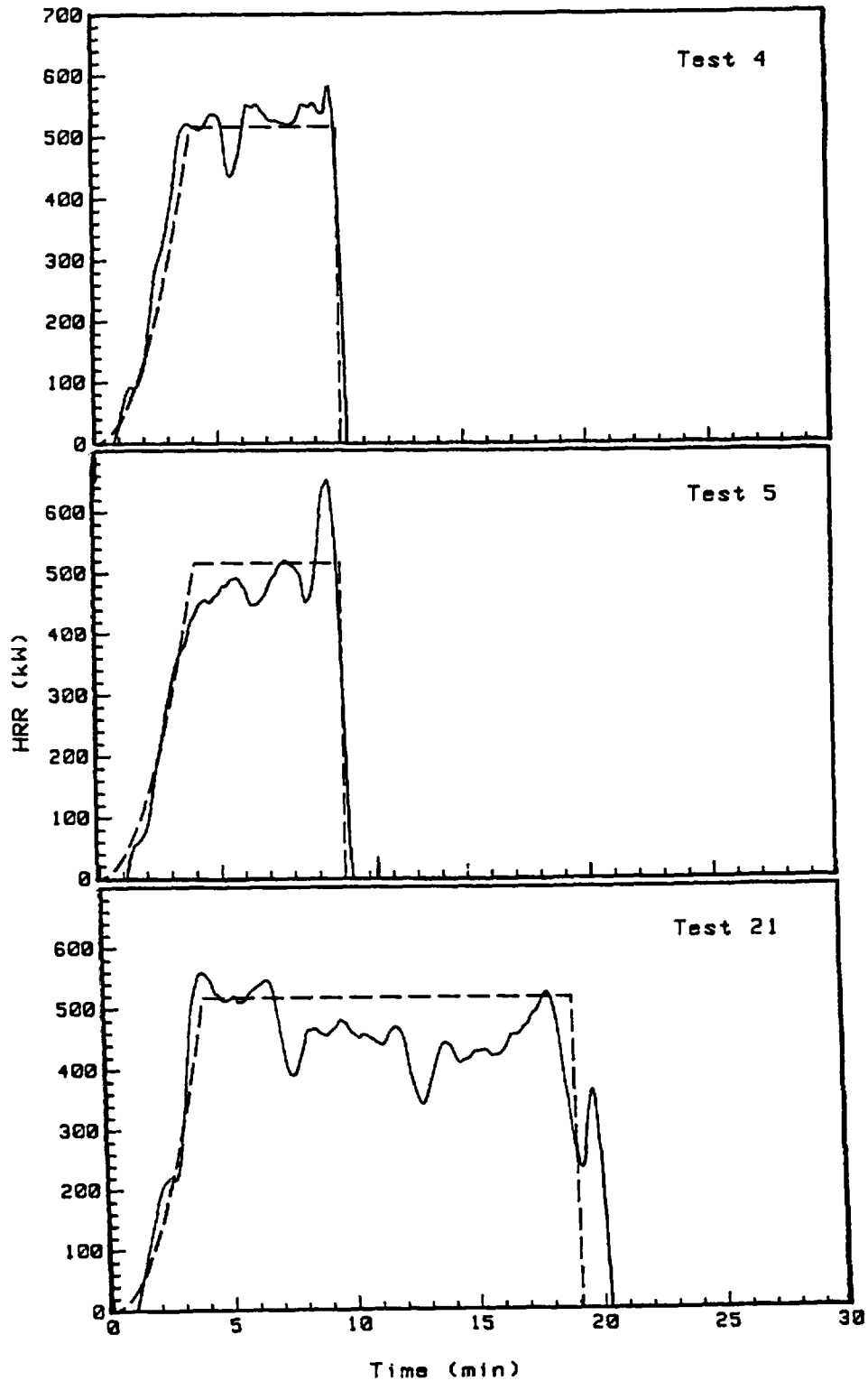


Figure 6: Heat Release Rates Calculated Based on Generation Rate of Carbon Dioxide for Tests 4, 5, and 21.

Figures 7 through 11 show three-dimensional plots of temperature versus the plan view location within the enclosure for each of the five planes at 5 and 10 minutes after ignition. In these plots the point (X,Y) equals (0,0) is defined as the N-E corner of the enclosure. The "Y" axis extends along the east wall (from zero to 40 feet). The "X" axis extends along the north wall (from zero to 60 feet). In these plots the thermocouple located directly above the fire at highest level (.98 x H) was artificially added to the data at each of the other four levels. This thermocouple was the only thermocouple located directly above the fire. By artificially attributing this thermocouple to all five levels one introduces an indication of the presence of the fire plume that would not otherwise be visible. Actual temperatures in the fire plume at these lower levels would certainly have been higher than those measured near the ceiling.

It is also possible to generate a variety of two-dimensional plots of the test data. The first examples of the two-dimensional plotting capabilities are shown in Figure 12. This figure shows the smoke optical density at two levels of the Sector 2 instrument tree (at the very center of the enclosure) during Tests 4, 5, and 21. Note that for each elevation and during each test the optical density would remain a zero (indicating no smoke at that location) for a given period and then rather suddenly and sharply rise to levels indicative of extremely poor visibility conditions. This data is in agreement with observations made during the testing. In each case a well-defined smoke layer was observed to form in the enclosure and descend through the room. Even as the layer descended past the level of the ventilation inlets (at 16 feet or 4.9 m), the layer was observed to remain quite well defined with a definite interface apparent.

It is interesting to compare the results of Tests 4 and 5. These tests differed only in that Test 4 used a low-ventilation rate (1 ch/hr), while Test 5 used a high-ventilation rate (10 ch/hr). In Test 5 the smoke layer actually reaches the 6-foot level nearly 1.5 minutes earlier than in Test 4. While the smoke layer descends more quickly at the higher ventilation rate, it is also apparent that the density of the smoke is lower under the higher ventilation conditions. Even so, using correlations developed by Rasbach, estimated visibility distances at the Sector 2, 6 ft. elevation location during Test 5 following passage of the smoke layer are on the order of 1.0 - 1.5 meters depending on lighting conditions [8].

Figures 13 and 14 illustrate a commonly encountered data presentation technique. These plots show the vertical temperature profile as measured by the aspirated

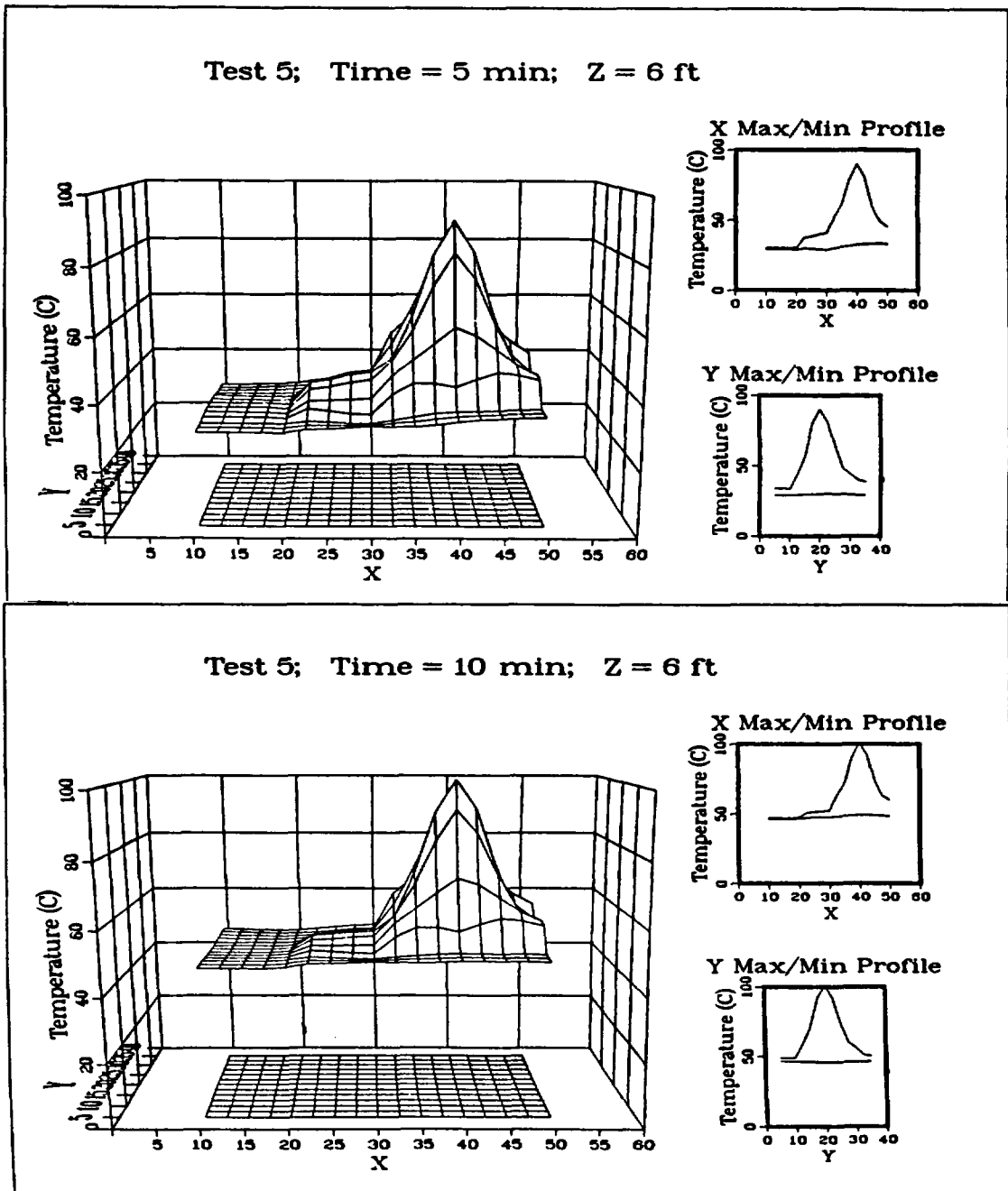


Figure 7: Three-Dimensional Plot of Temperature Versus Plan View Location for the 6-Foot Elevation at 5 and 10 Minutes After Ignition in Test 5.

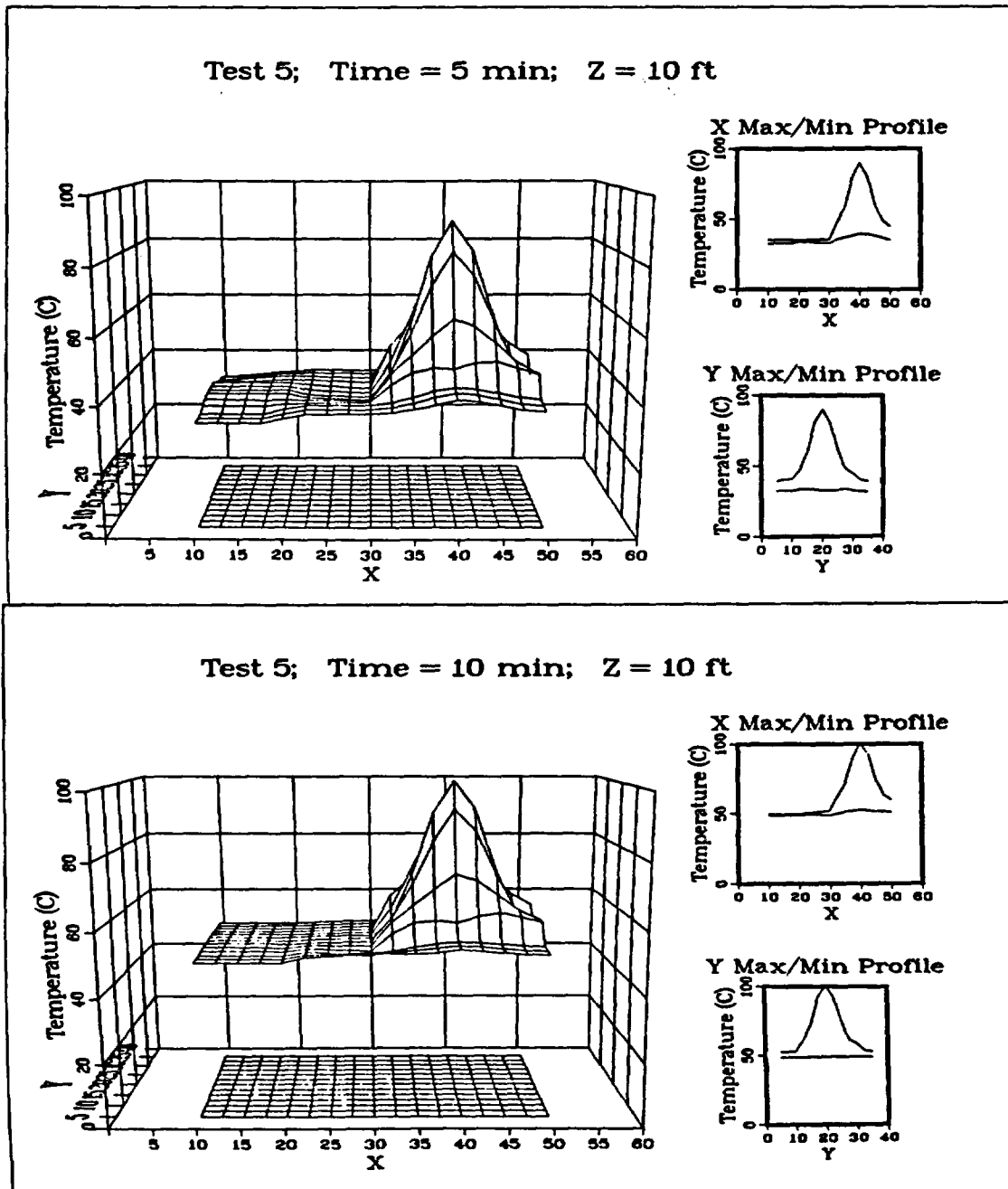


Figure 8: Three-Dimensional Plot of Temperature Versus Plan View Location for the 10-Foot Elevation at 5 and 10 Minutes After Ignition in Test 5.

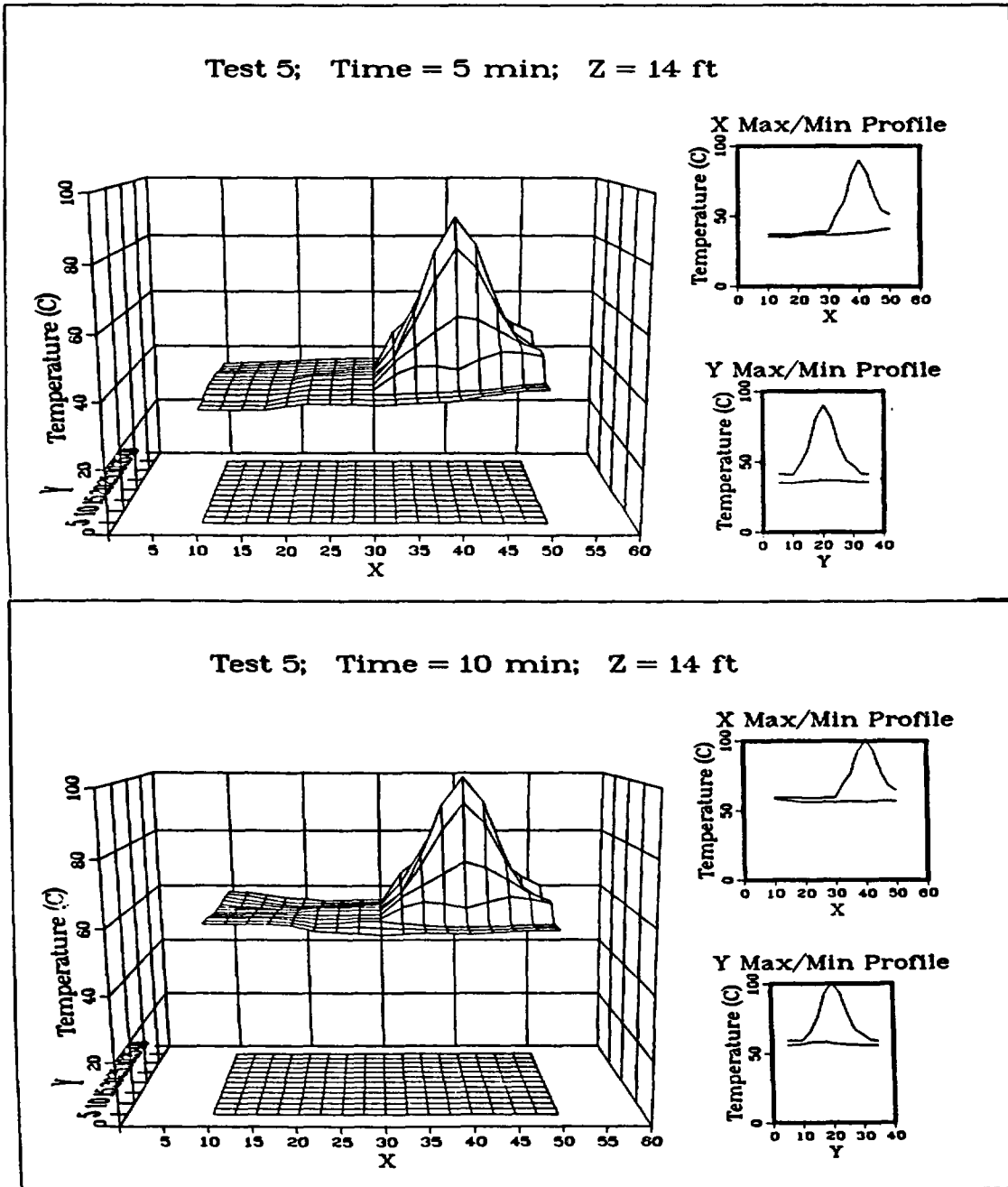


Figure 9: Three-Dimensional Plot of Temperature Versus Plan View Location for the 14-Foot Elevation at 5 and 10 Minutes After Ignition in Test 5.

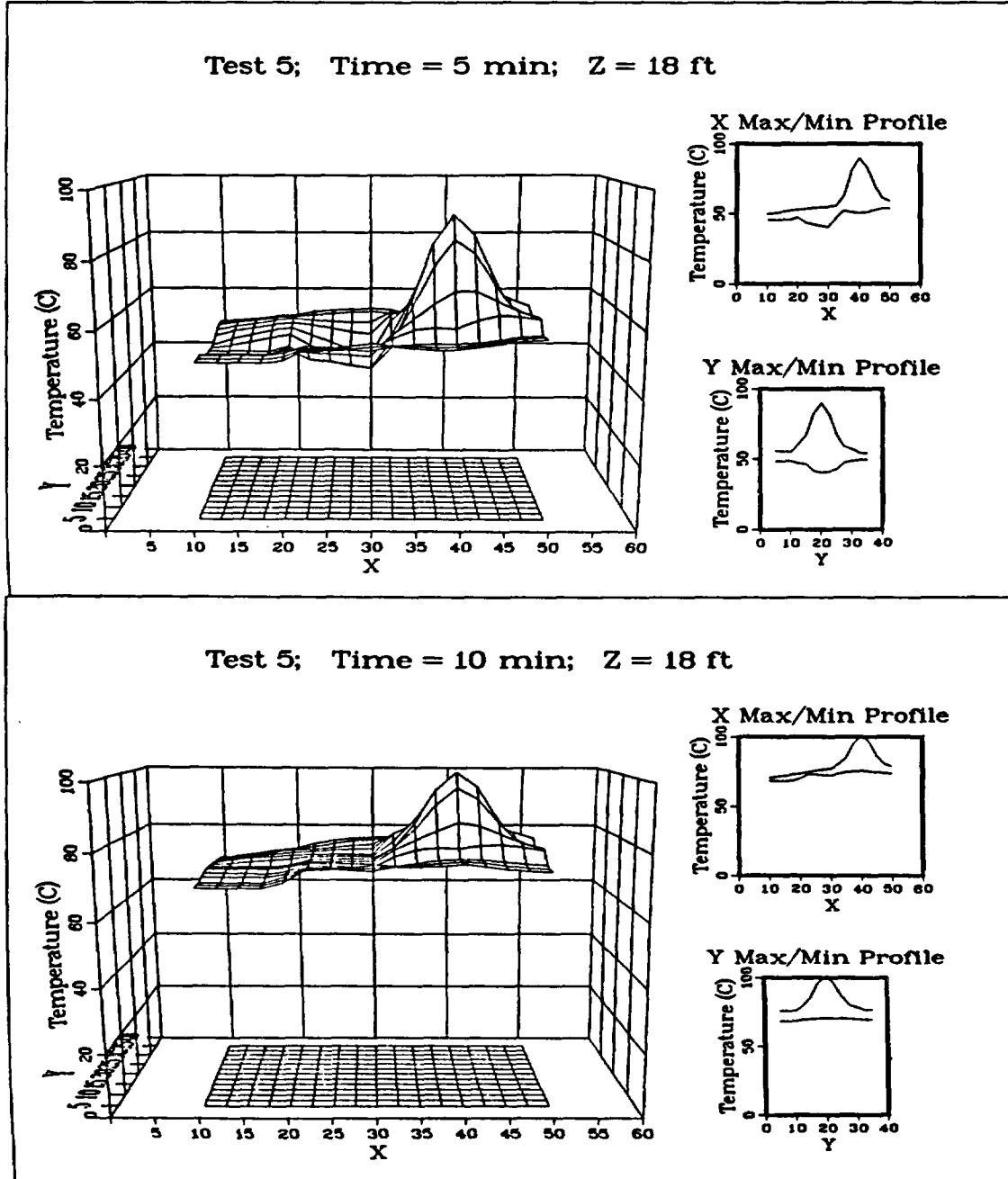


Figure 10: Three-Dimensional Plot of Temperature Versus Plan View Location for the 18-Foot Elevation at 5 and 10 Minutes After Ignition in Test 5.

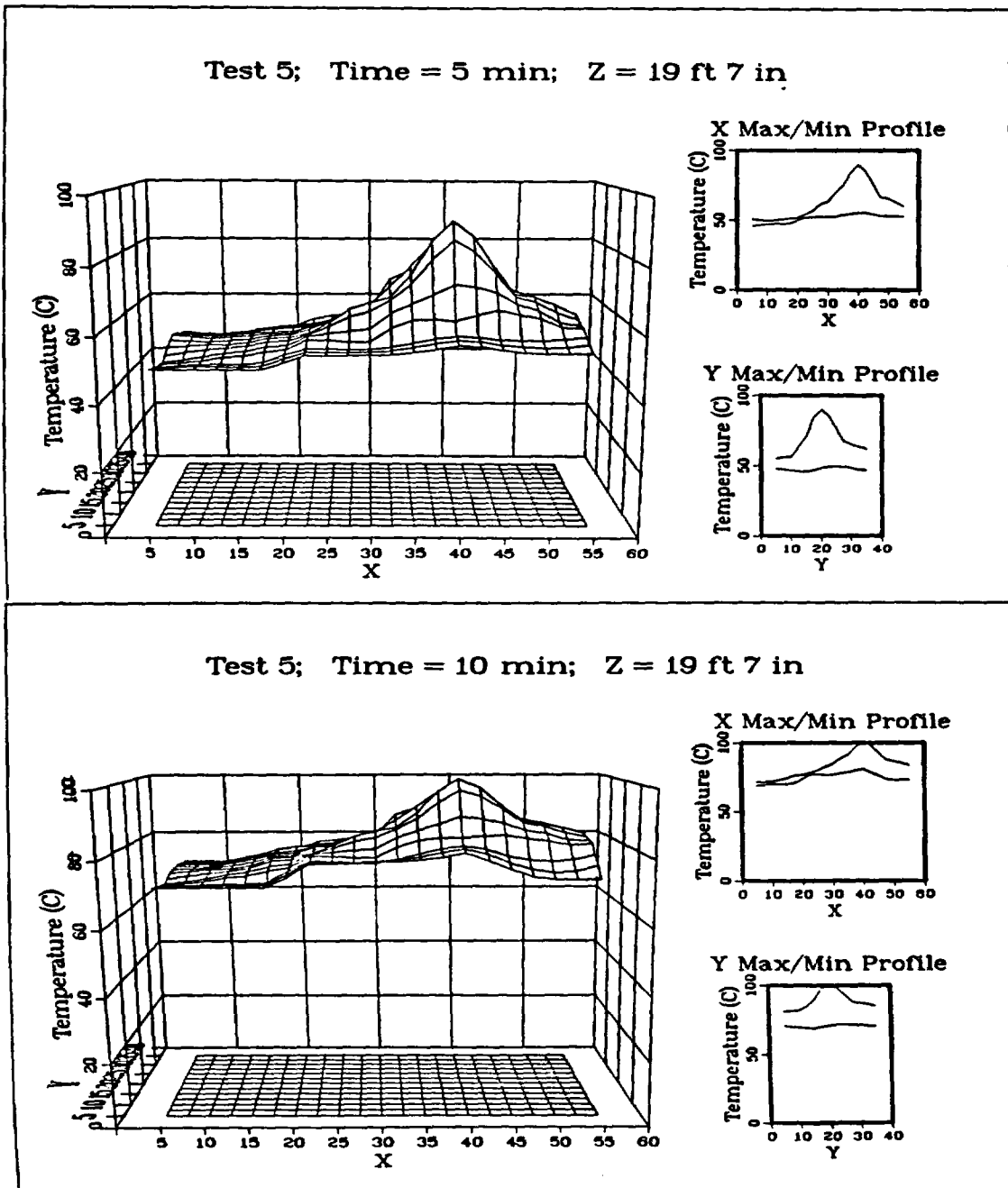


Figure 11: Three-Dimensional Plot of Temperature Versus Plan View Location for the 19-Foot, 7-Inch Elevation at 5 and 10 Minutes After Ignition in Test 5.

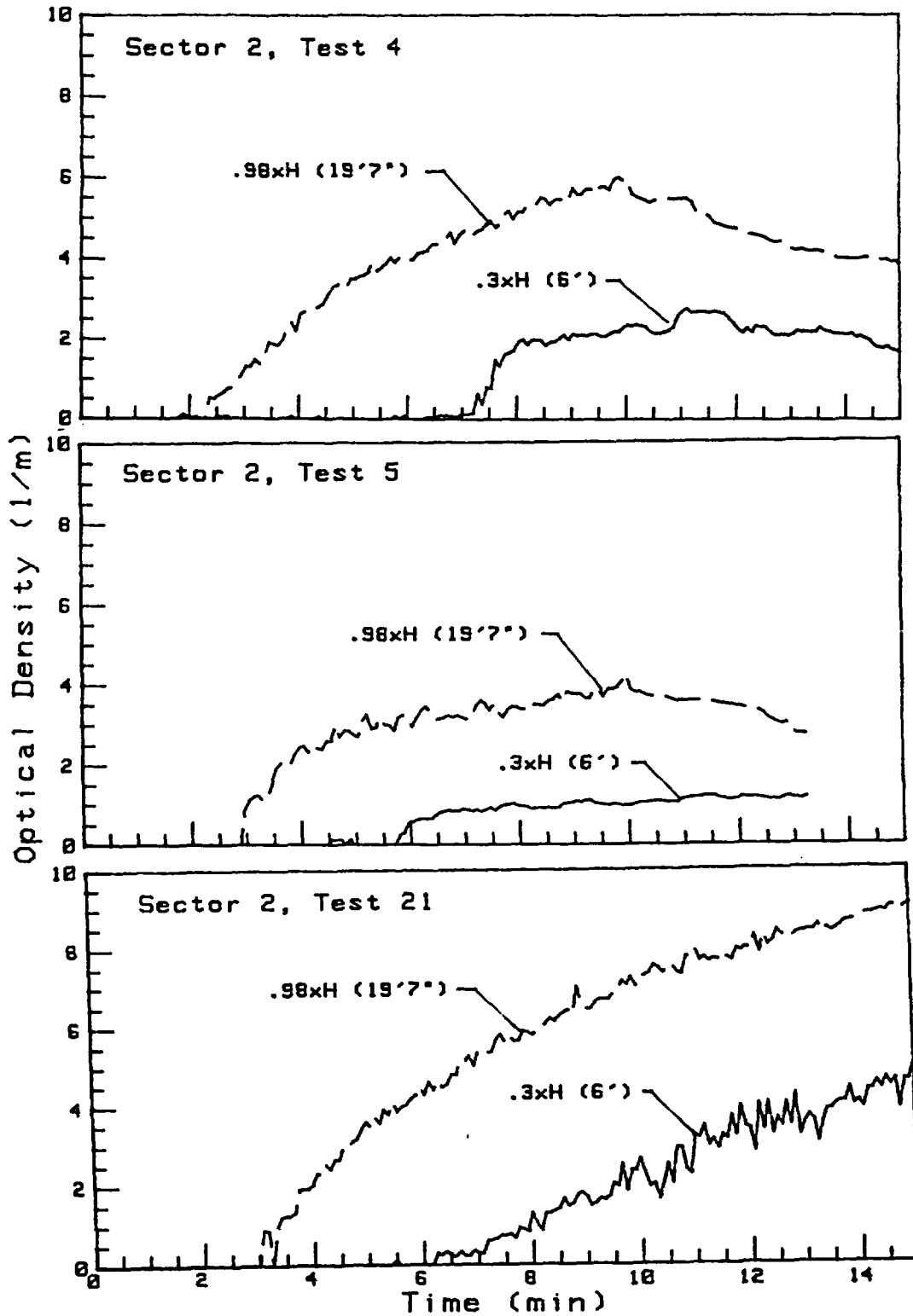


Figure 12: Smoke Optical Density to Blue Light at Each of Two Elevations on Sector 2 Instrument Tree During Tests 4, 5, and 21.

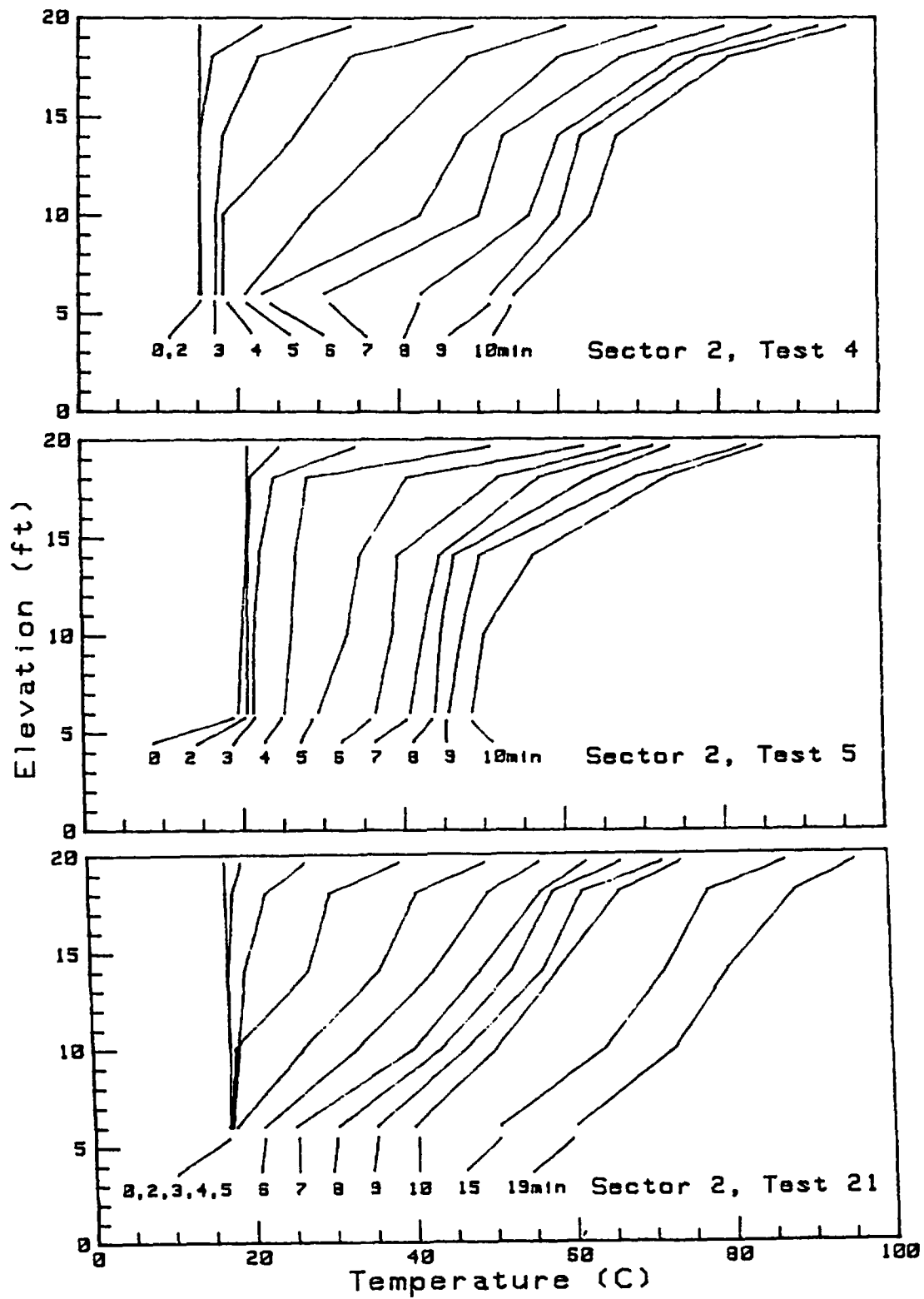


Figure 13: Vertical Temperature Profile at Sector 2 Location During Fire Growth and Fire Steady-State Periods of Tests 4, 5, and 21.

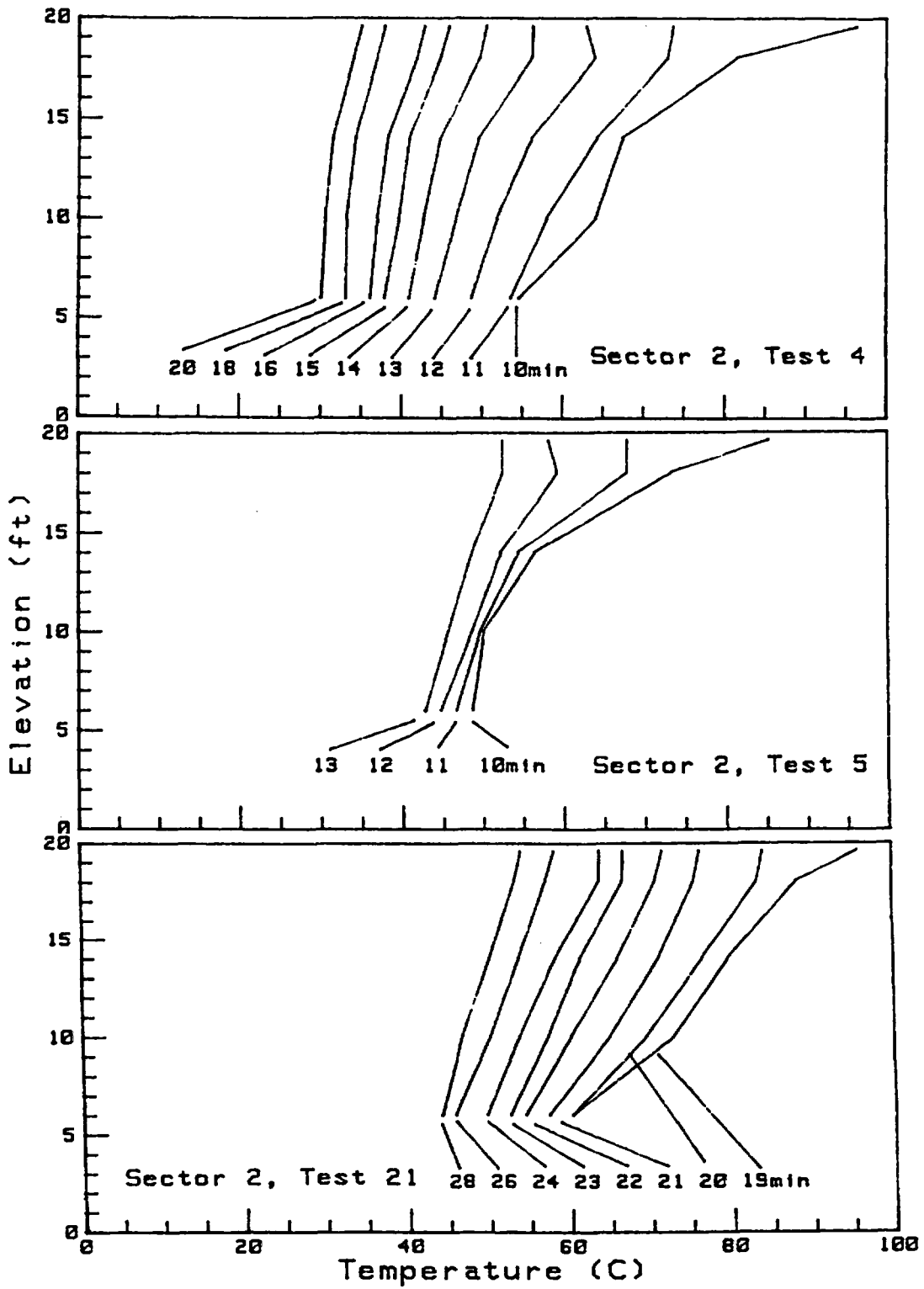


Figure 14: Vertical Temperature Profiles at Sector 2 Location Following Fire Extinguishment in Tests 4, 5, and 21.

thermocouples on the Sector 2 instrument tree during Tests 4, 5, and 21. Figure 13 presents data for the time period from fire ignition to fire burnout. Figure 14 shows data for times after fire extinguishment. Note that the ventilation system shut down because of overheating at 9 minutes into Test 5.

The plots in Figure 13 show some rather interesting features. The plot for Test 21 shows the type of temperature development one normally expects to see during an enclosure fire. Temperatures at each level remain at ambient for a given time period and then, starting at the highest level, temperature readings start increasing. This behavior is consistent with the development of a hot layer that descends through the room. The times at which the highest and lowest level temperatures first deviate significantly from ambient are also consistent with the time at which the smoke layer passes these points as shown in Figure 12.

This type of hot layer development is not as clearly indicated for Tests 4 and 5. In Tests 4 and 5 the smoke layer is observed to pass the 6-foot level at approximately 7 and 6 minutes after ignition, respectively, as shown in Figure 12. However, unlike Test 21, in Test 4 by 7 minutes temperatures at the 6-foot level had risen approximately 15°C. In Test 5 by 5 minutes temperatures had risen approximately 10°C above ambient. These temperature rises prior to passing of the hot smoke layer represent a significant fraction of the total temperature rise for that point over the full length of the test. This heating of the enclosure air prior to hot layer passage can only be accounted for by absorption of thermal radiation. In the case of Test 21 the fire was within a heavy steel cabinet that presumably absorbed a large fraction of the radiative heat released by the fire, particularly that which would normally have been directed toward the center of the enclosure. However in the case of Tests 4 and 5 the fire was placed in the open with no shielding. In most analyses air is considered transparent to thermal radiation. The presence of water vapor in the atmosphere can, however, result in significant absorption of thermal radiation. In Tests 4 and 5 ambient relative humidities were 60 and 65 percent respectively. Using correlations outlined by Siegel and Howell [5], estimated total absorptivities for the enclosure air are on the order of 23-25 percent.

Thus the data indicates that radiative heating of the enclosure air is a significant effect under certain test conditions. Indeed for the case of Tests 4 and 5 the preheating of the air prior to passage of the hot layer results in a significant fraction of the total temperature

rise throughout the test. The data does indicate that for the time period between 7 and 8 minutes in Test 4 and for the time period between 5 and 6 minutes in Test 5 the temperature change at the 6-foot level is greater than during any other one-minute period. This is indicative of a hot layer passing, though the temperature rise due to the hot layer passage is nearly undetectable. Other methods, such as differentiation of temperature profiles and plotting of the difference between layer temperatures, have been attempted but because of the "noise" in the data have not been successful in detecting the hot layer passage for Tests 4 and 5.

One method that has been useful in highlighting certain fire developments under the open fire conditions is comparison of bare-bead and aspirated thermocouple measurements. Figure 15 shows this data for the Sector 2 6-foot elevation location during Test 4. The first plot shows the actual temperature data as measured by both the bare-bead and aspirated thermocouples at that location. The second plot shows the difference in the measured temperature for these two probes. The bare-bead thermocouple is subject to distortion of the measured value because of absorption of thermal radiation. The aspirated thermocouple is shielded from radiative heat flux and provides a measure of the true gas temperature.

As is clearly demonstrated in the second plot, developments in the fire and enclosure environment are clearly reflected in the difference in temperature measurements. During the first 4 minutes, while the fire is growing from zero to 516 kW, the difference in measured temperature rises along a similar growth profile to approximately 8°C. This difference is maintained during the steady-state phase until approximately 7.5 minutes after ignition when the measured difference drops to approximately 6°C. As shown in Figure 12 this time corresponds to the passage of the smoke layer at this location. At 10 minutes, when the fire is extinguished, the measured temperature difference quickly dropped to zero. Thus the growth in fire intensity (and hence the radiative heat flux levels), the reduction in radiative heat flux caused by attenuation by the smoke layer, and extinguishment of the fire are clearly reflected in these measurements.

Figure 16 shows the same data for Test 5. Here again the same behavior is clearly evident. Figure 17 shows this data for Test 21. In this case the behavior is rather different. As the radiative heat flux from the fire source to this location is rather well shielded, the behavior shown for Test 21 probably is due to radiative heat flux from the smoke layer itself rather than from the fire.

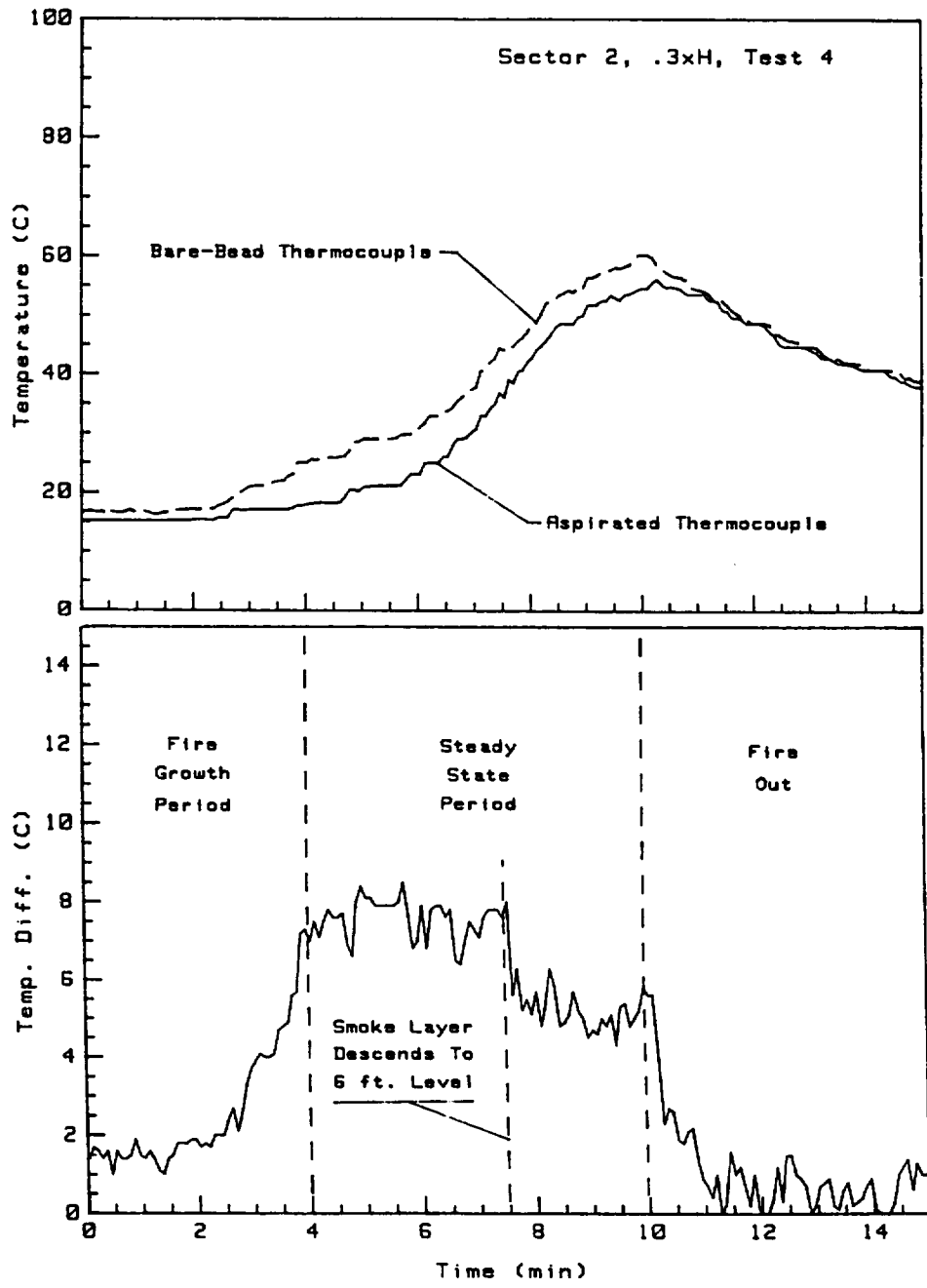


Figure 15: Data From Bare-Bead and Aspirated Thermocouples at Section 2, 6-Foot Location During Test 4.

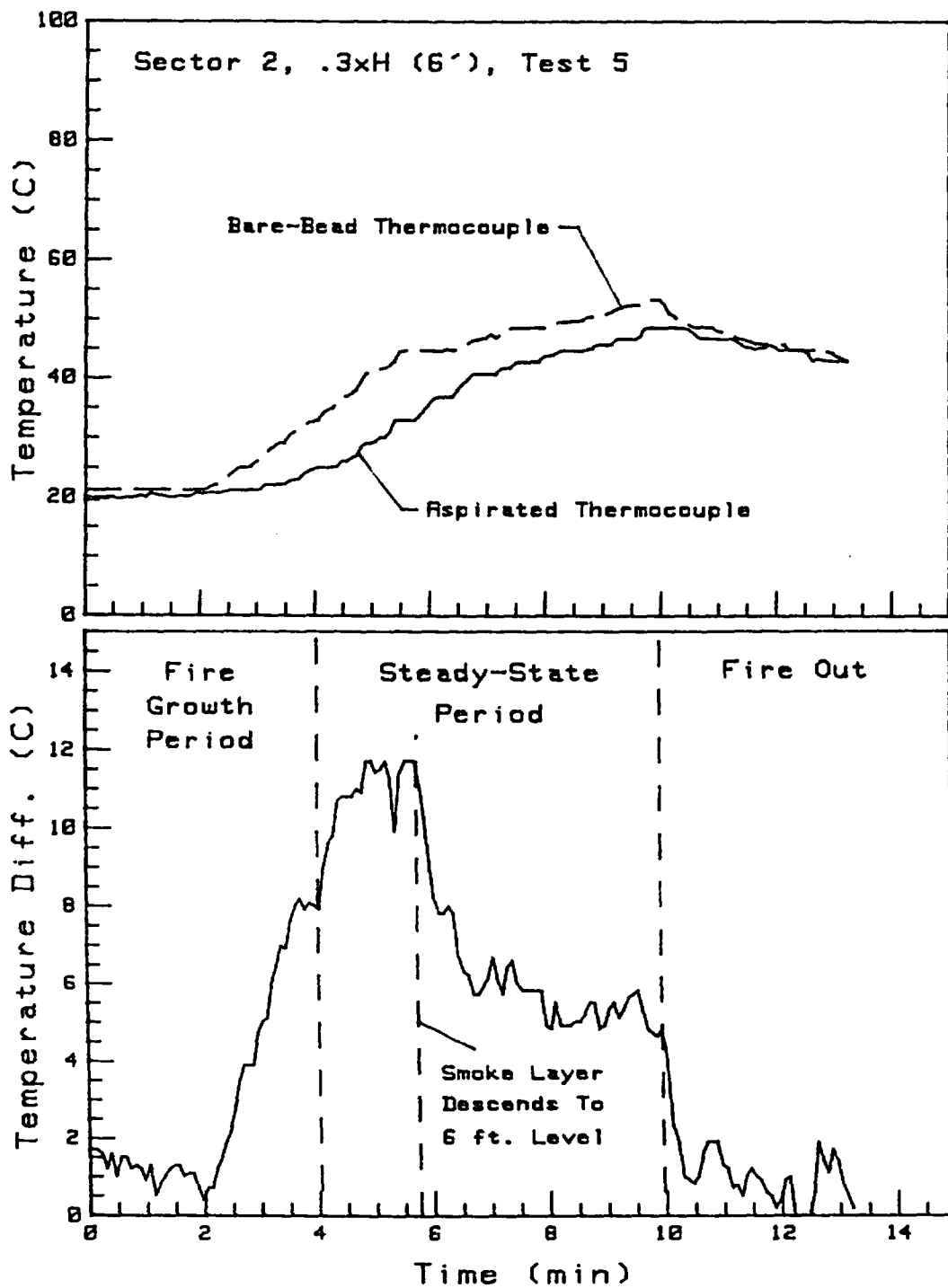


Figure 16: Data From Bare-Bead and Aspirated Thermocouples at Section 2, 6-Foot Location During Test 5.

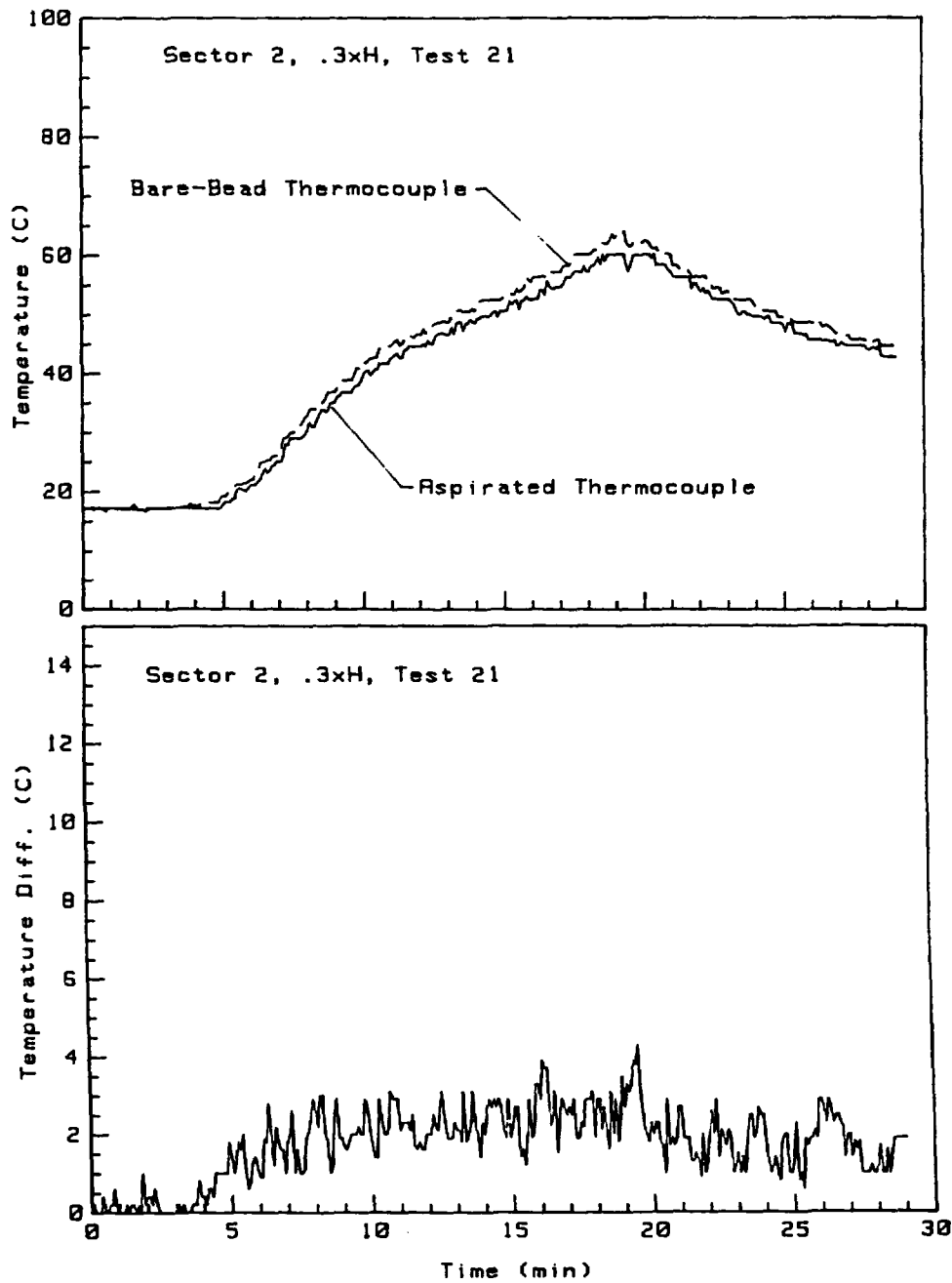


Figure 17: Data From Bare-Bead and Aspirated Thermocouples at Section 2, 6-Foot Location During Test 21.

Further analysis of the test data in the future should be helpful in defining the causes of the behavior shown in Figure 17.

Quantification of radiative heat flux levels in the enclosure can be accomplished through analysis of the data from the large and small sphere calorimeters installed at each of nine locations in the enclosure. By using both large diameter (12.7 mm) and small diameter (6.35 mm) sphere calorimeters in tandem, it is possible to determine both the radiative and convective fractions of the total net heat transfer rate as well as the convection heat transfer coefficient and bulk flow velocity. The calculation procedure has been described by Newman and Hill [1]. Because the calculation involves radiative heat transfer modeling, fourth-order and fourth-root terms are introduced. This makes the calculation process extremely sensitive to temperature fluctuations and "noise" in the data. In order to obtain useful results, it was found that curve fitting of the raw temperature data prior to calculation was necessary. Ninth-degree polynomial curves were fit to the data for the large and small calorimeters and true gas temperatures using a linear parameter estimation routine based on ordinary least squares techniques as described by Beck and Arnold [6]. The results of this curve fitting procedure are illustrated in Figure 18, which shows both the raw data and curve fit approximations for the Sector 2, 6-foot location during Test 5.

Using the curve fit data shown in Figure 18 and the calculation process described in Reference 1, the equivalent radiative environment temperature was calculated as shown in Figure 19. Based on this temperature the radiative and convective heat flux levels can be calculated as shown in Figure 20. Note that here again fire and enclosure environment developments are reflected in the heat flux measurements. Total and radiative heat flux levels increase through the growth phase of the fire with convection acting to cool the calorimeters. Following descent of the smoky hot layer to the 6-foot level (at approximately 5.75 minutes), radiative heat flux levels drop significantly, though they remain predominate. This location happens to be rather close to the fire (approximately 10 feet from the plume centerline). At locations more remote from the fire radiative heat flux levels drop.

The behavior shown in Figure 20 is consistent with the expected results. Initially both spheres are at approximately the same temperature, and as they are each exposed to the same environment, the radiative heat flux levels are the same for both spheres. As the test progresses, the flux

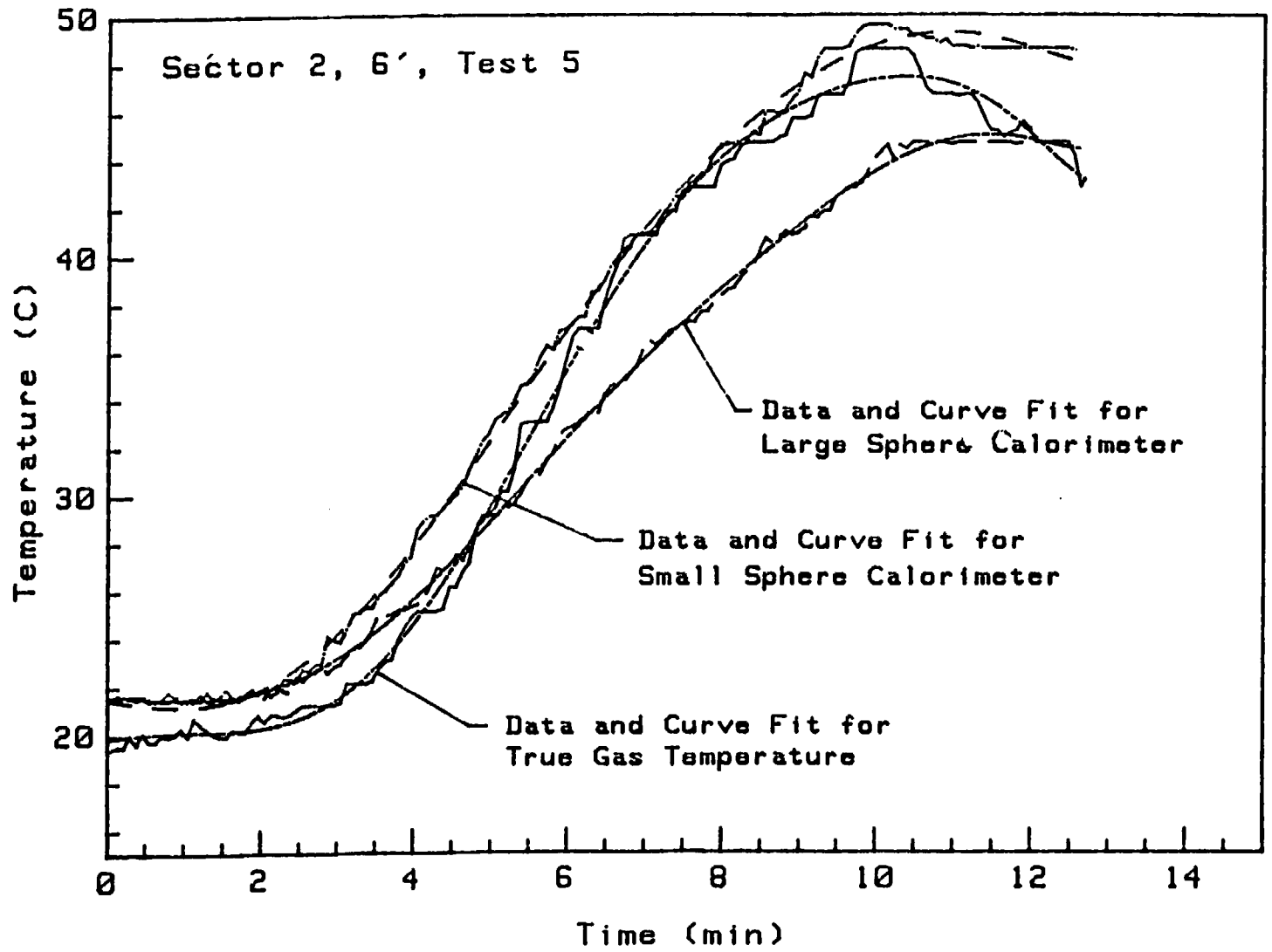


Figure 18: Raw Data and Curve Fit for Sector 2, 6 Foot Location Sphere Calorimeter Processing During Test 5.

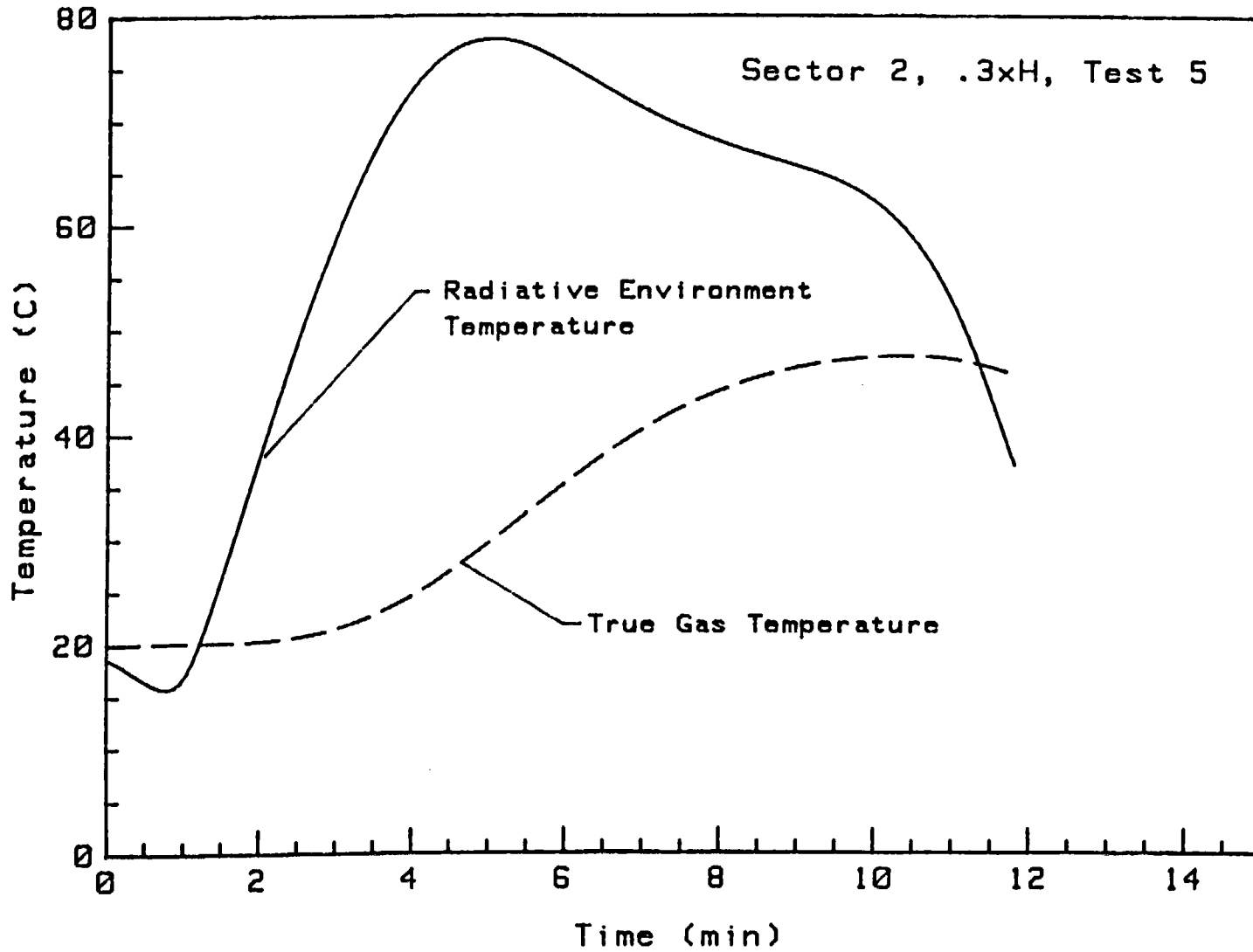


Figure 19: Equivalent Radiative Environment Temperature Derived Based on Sphere Calorimeters at Sector 2, 6 Foot Location During Test 5.

Sector 2, .3xH, Test 5

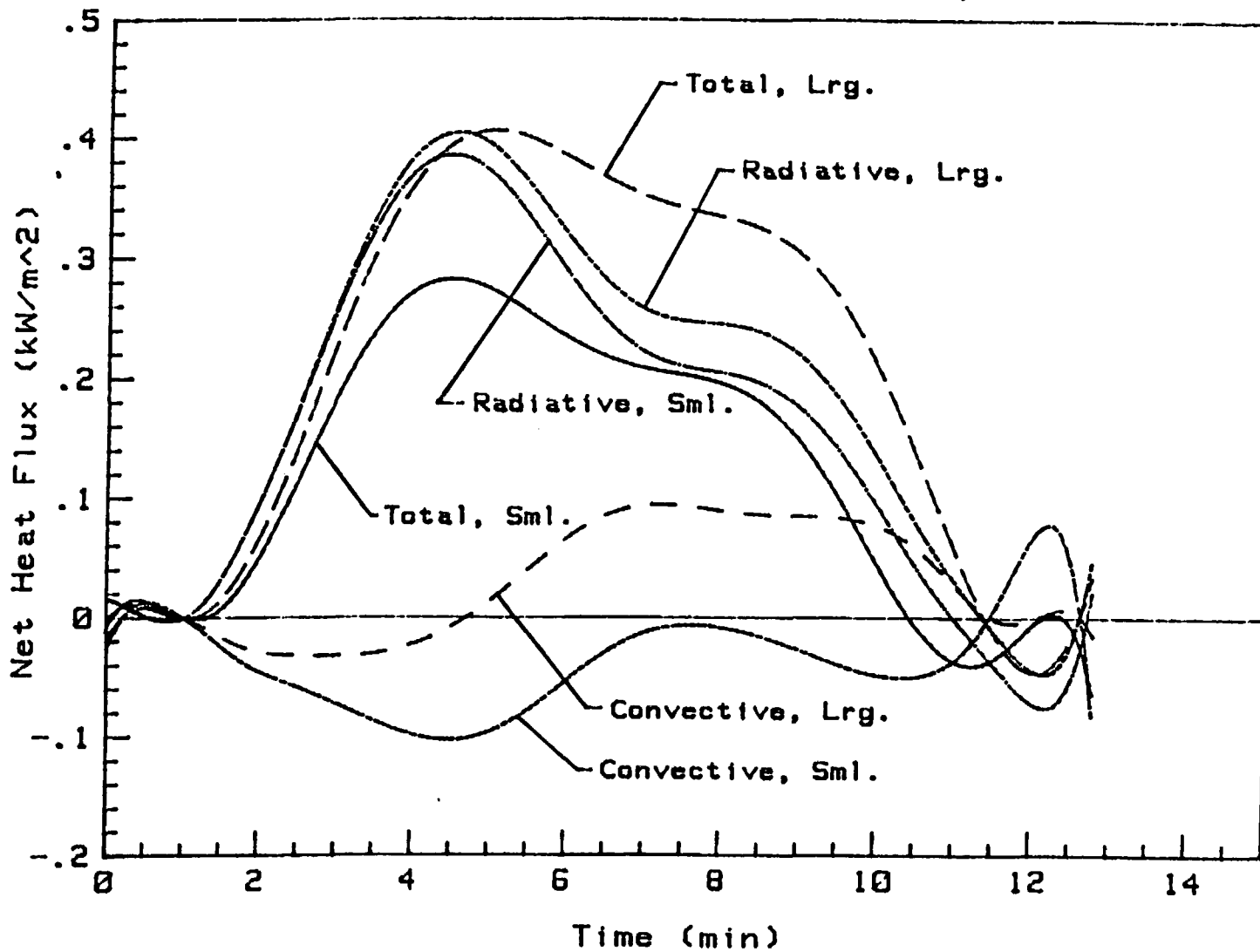


Figure 20: Net Heat Flux Levels for Sphere Calorimeters at Sector 2, 6 Foot Location During Test 5.

enclosure air. Humidity levels will clearly play a role in determining the significance of this effect. Second, for the conditions present during these tests, hot layer temperatures remained quite low compared to other test efforts. Room size and ventilation conditions appear to have a major effect on the hot layer development. Third, the data seems to indicate that hot layer development below the level of the forced ventilation inlets is significantly different from that which occurs above the inlet duct level. In the zone modeling of the forced ventilation enclosure fire, it may be appropriate to split the usual hot layer into two parts: one above the ventilation inlets and one below. Fourth, while the higher ventilation rates appeared to result in somewhat less dense smoke levels, the higher rates also contributed to faster descent of the smoke layer. The high ventilation rate of 10 air changes per hour was not effective in maintaining a clear environment in the enclosure. In virtually all tests (all those other than the methanol pool fire tests) smoke densities were high enough to cause extremely poor visibility conditions throughout the room within 10 minutes of fire ignition.

Further analysis of the test data should help to more clearly define the effects of various parameters on these and other factors related to fire environment development in a large enclosure under forced ventilation. Further information on the availability of data may be obtained through Sandia National Laboratories or through the U.S. Nuclear Regulatory Commission.

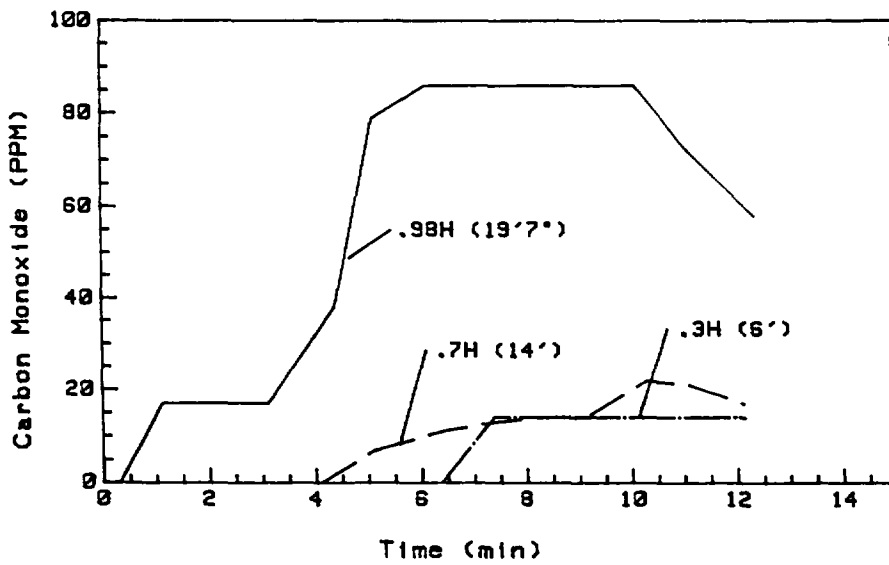
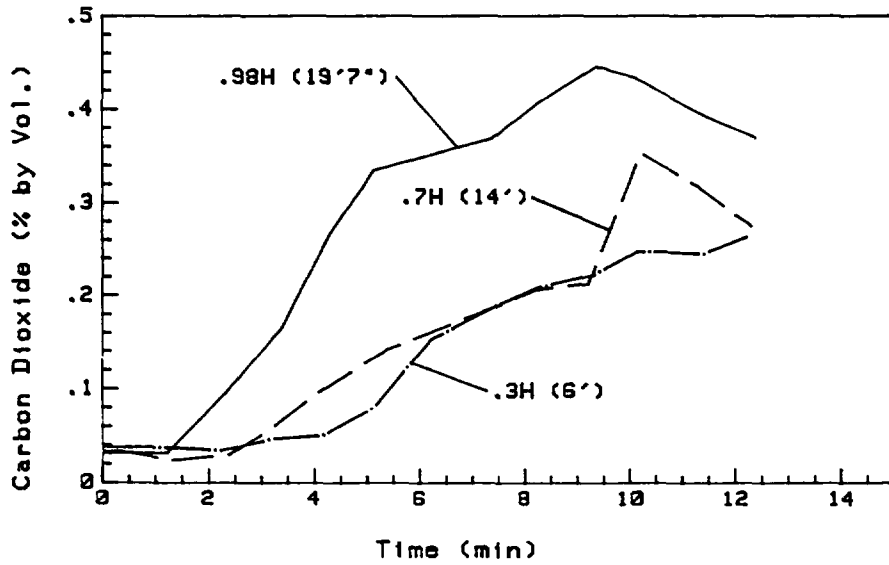


Figure 21: Carbon Dioxide and Carbon Monoxide Concentrations at Sector 2 During Test 5.

OMIN2.RC

APPENDIX A - TEST FACILITYEnclosure

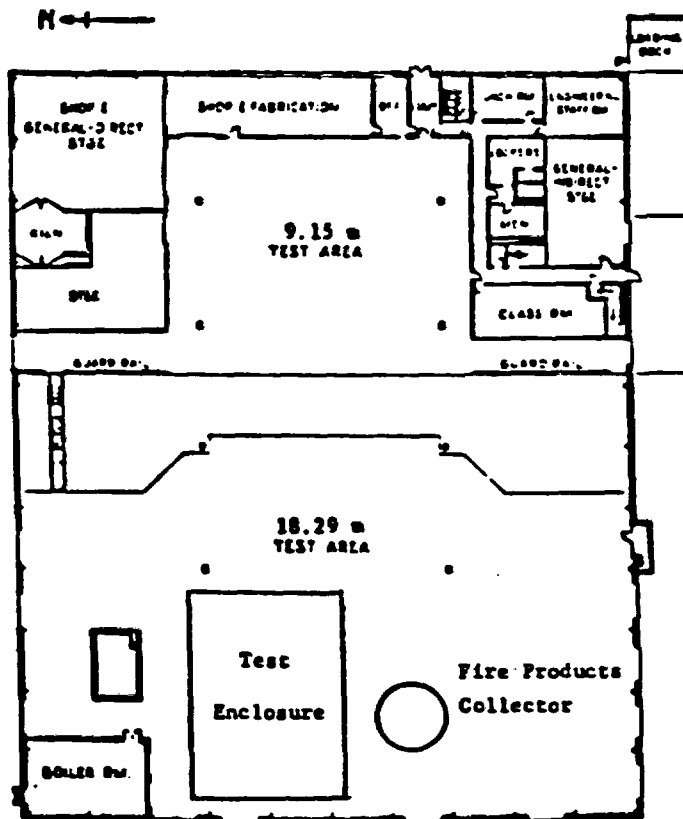
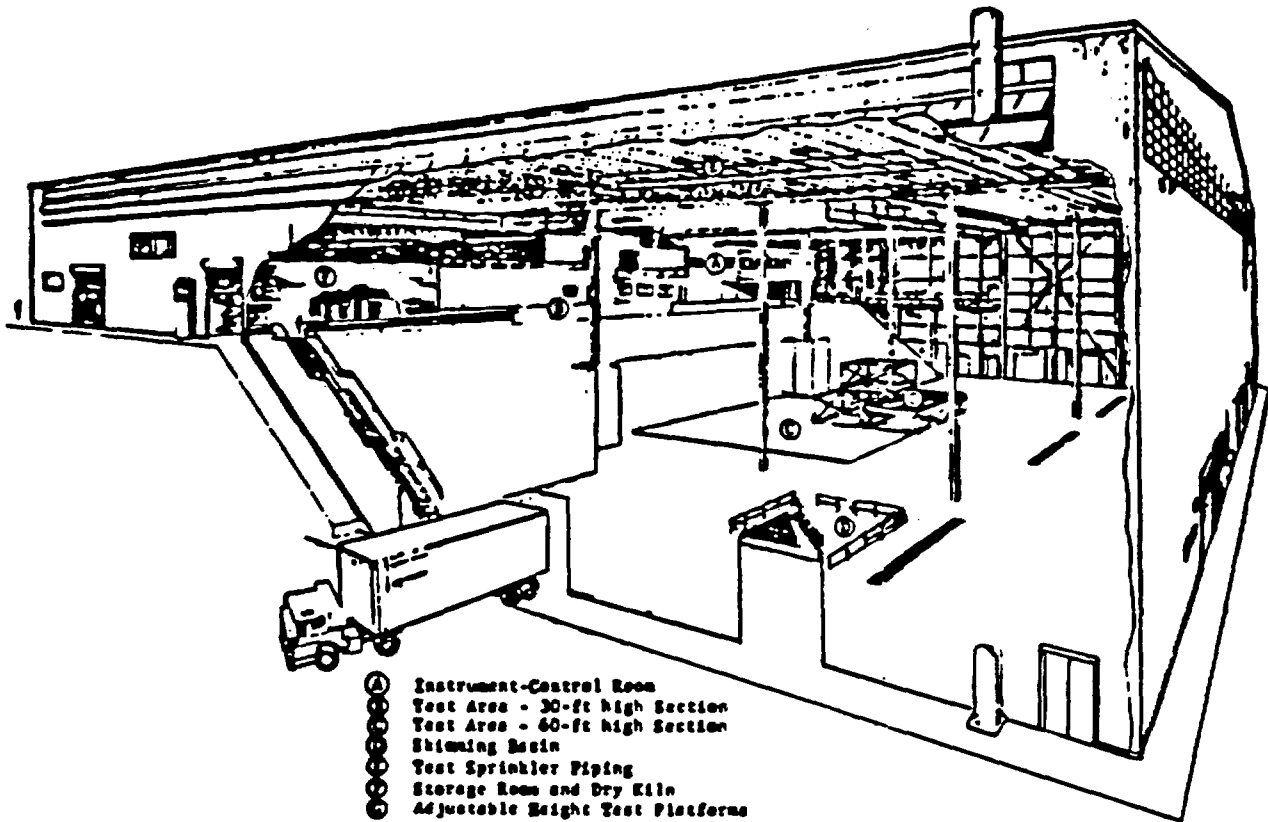
A pictorial of Factory Mutual (FM) Test Center and a layout showing the fire test enclosure are presented in Figures A-1 and A-2. The enclosure is built within the 18.29-m test site* of the FM Test Center and measures 18.28-m x 12.19-m x 6.10-m (L:W:H = 3:2:1). The enclosure walls are composed of 1.22-m x 2.44-m (4-ft x 8-ft) panels of Marinite I** having a thickness of 25 mm (1 in.). However, the ceiling panels were cut to measure 1.22-m x 1.22-m in order to ease the installation process. The panels are securely fastened with lag screws to an external framework constructed of 50-mm x 150-mm (2-in. x 6-in. nominal dimensions) framing lumber. It should be noted that oversized holes were drilled in the panels and washers provided for the lag screws in order to minimize both mechanical and thermal cracking effects. Additional supports and braces are provided between wall studs, at the ceiling corners, and over doorways and observation windows. Seams formed by the Marinite I panels are backed by the wooden framework, and a bead of high temperature silicone sealant (i.e., RTV - Room Temperature Vulcanization) is provided between all seams. The RTV will allow the panels to expand when subjected to elevated temperatures and help maintain a sufficiently airtight environment. The ceiling is suspended from five 12.9-m, open-web steel joists which are supported and held in place by the N and S walls. This type of support system will allow the enclosure interior to be free of vertical obstructions. Observation windows (wire glass) are located on the N and S walls of the room for both visual and photographic monitoring of test events and access doors are provided along the N, E, and W walls. Later in the test program, the enclosure will be modified in order to provide half rectangular, "L"-shaped and 4.3-m suspended ceiling height configurations.

* The FM Test Center has two primary heights beneath a single large ceiling. One section is 9.14-m high (~ 30 ft) and the other is 18.29-m high (~ 60 ft)

** Marinite I is a registered trademark of the Johns-Manville Corporation.

Ventilation

The enclosure is equipped with a ventilation system (see Figure A-3) comprised of a belt-driven centrifugal-forced draft blower, capable of delivering an air flow of $3.8 \text{ m}^3/\text{s}$ (standard conditions) or approximately 10 room changes/hr. The fan housing is provided with an adjustable vane-type baffle plate which controls the influx of air to the enclosure. The air stream will be passed through a long run of 0.61-m diameter, galvanized steel duct which will allow for an air-mass flow rate measurement by means of an orifice plate. After passing through a series of 90° bends, the flow will enter a "T"-shaped distribution box with damper control, located on top of the enclosure. The air will then flow into two rectangular-shaped trunk lines which will distribute $1.9 \text{ m}^3/\text{s}$ of air through three inlet diffusers per trunk line. The diffusers measure $0.46 \text{ m} \times 0.46 \text{ m}$, and the diameter of each trunk line has a series of reductions so that the flow of air through each diffuser is about $0.63 \text{ m}^3/\text{s}$ at $\sim 3 \text{ m/s}$. These diffusers will offer four-way deflection and damper control to help balance the system (i.e., $\sim + 31 \text{ Pa}$ or $1/8 \text{ in.}$ water above atmosphere inside the enclosure). An exhaust vent assembly ($\sim 0.61\text{-m} \times 1.83\text{-m}$, open-grille) is located on the ceiling near the E wall and is equipped with a damper control. At this point the efflux will be ducted over to the FM Fire Products Collector (see Appendix B) where additional measurements will be made.



FLOOR PLAN

FIGURE A-1 FM TEST CENTER (TOP) AND TEST ENCLOSURE LOCATION (BOTTOM)

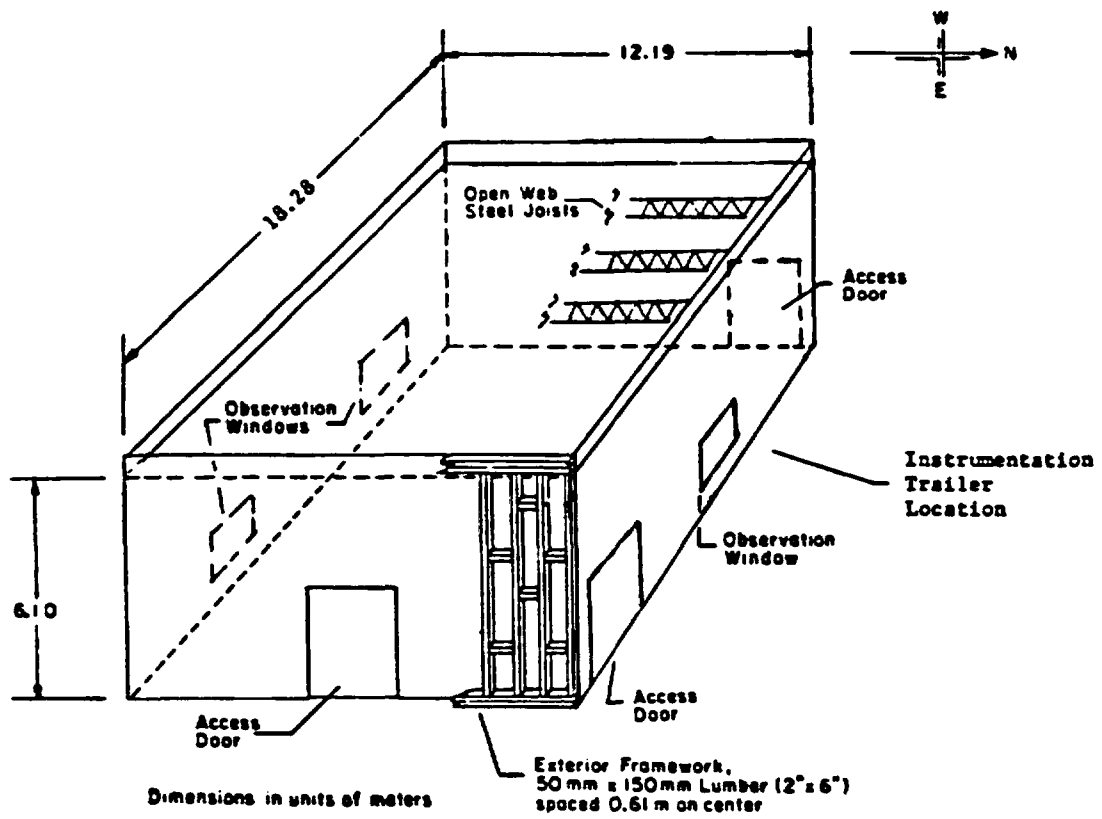


FIGURE A-2 THREE-DIMENSIONAL VIEW OF TEST ENCLOSURE

A-5

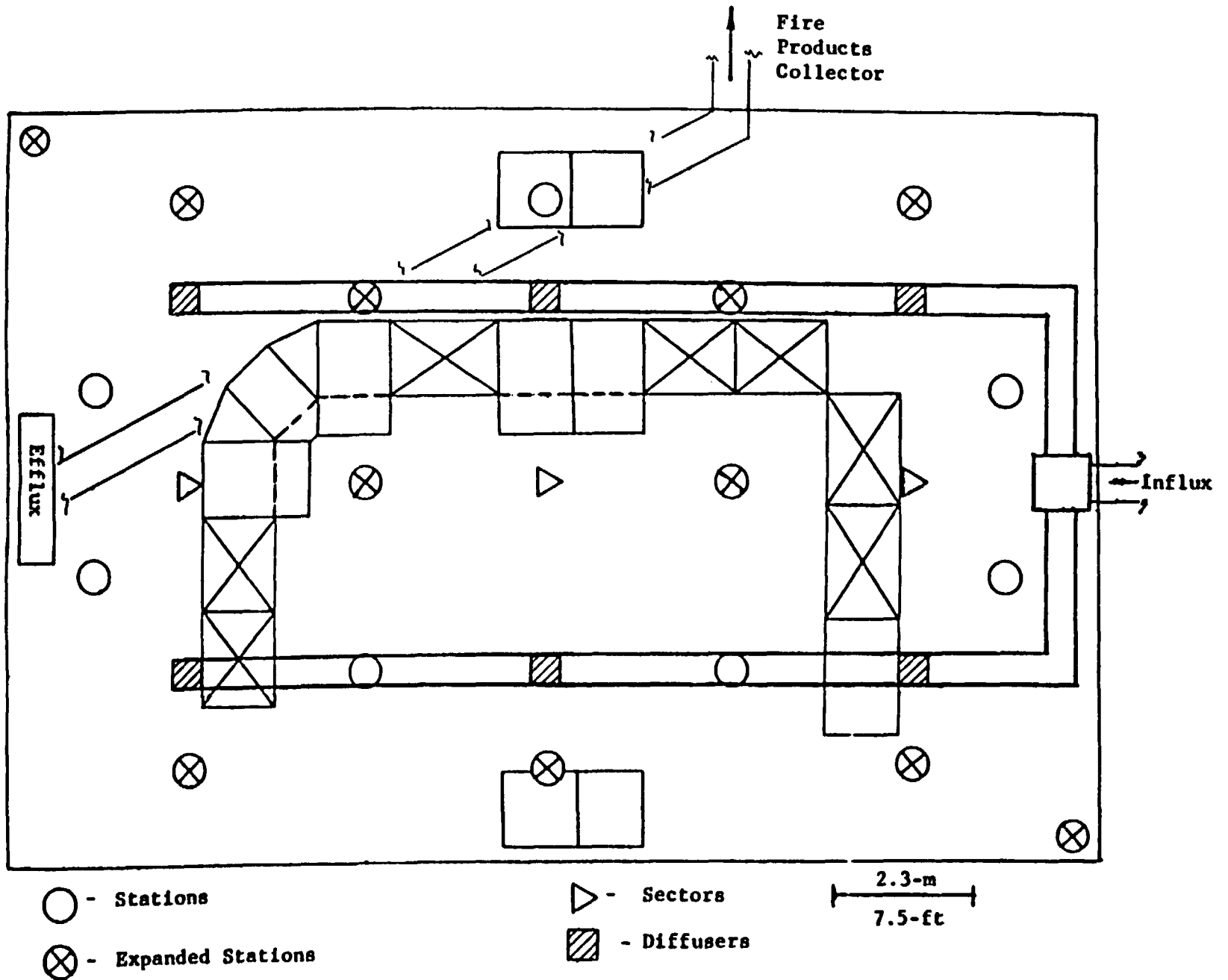


FIGURE A-3 VENTILATION SYSTEM LAYOUT WITH RESPECT TO INSTRUMENTATION AND CABINETS

FACTORY MUTUAL RESEARCH CORPORATION

OMIN2.RC

APPENDIX B - INSTRUMENTATION

Up to a total of 249 data channels for each enclosure test (excluding demultiplexed gas channels, smoke detector channels, and channels required for the Fire Products Collector) will be monitored by a Hewlett-Packard, 1000F, computer-based data acquisition system. Thermocouple signal conditioning is provided for all low-level inputs. The system is used to collect data at high rates from Test Center experiments and provide draft plots or tables after a test. A magnetic tape transport is used to write tapes for transport to the Norwood analysis system. A fixed disk drive provides local storage for data and software. Of these 249 channels, 92 will be used for gas temperature measurements by bare-bead and aspirated thermocouples; 18 will be for temperature measurement associated with small and large sphere calorimeters; 69 will be for surface temperature measurements; 27 will be for cement-on heat flux sensors; 10 will be continuous or multiplexed CO, CO₂, O₂, and THC concentration measurements at 10 sampling locations; 18 will be gas velocity measurements; 8 will be optical density measurements by six smoke turbidimeters; 1 will be for mass loss rate measurement; and 6 will be for pressure measurements inside room doorway, inlet and outlet of the ventilations, and at the "cabinet".

As the instrumentation is described, references are made to diagrams presented in Figures B-1 to B-3 showing the location of the various instruments in the enclosure. A data channel map is given in Table B-I. Figure B-1 shows the ceiling instrumentation layout (view looking into enclosure). Figure B-2 gives one of the three vertical instrumentation configurations below each instrumentation sector on the ceiling. Figure B-3 gives the instrumentation layout for the enclosure walls.

Gas Temperature

Sixty-one bare-bead thermocouples made from 24 AWG chromel-alumel, stainless steel overbraided Kapton wire will be used on the ceiling (Figure B-1) and at the vertical locations (Figure B-2) of the enclosure; 31 aspirated thermocouples, designed by Newman and Croce^(A-1) will be used for true gas temperature measurements at various locations of the enclosure including ceiling and vertical locations.

Convective and Radiative Heat Fluxes

Convective and radiative heat fluxes will be calculated from the temperature measurements made with several small- and large-sphere calorimeters near the ceiling (Figure B-1) and at the vertical locations (Figure B-2). The specifications of sphere calorimeters and heat flux measurement techniques are given in Reference B-2. In addition, gas velocity can also be calculated from the temperature measurements made with the sphere calorimeters^(B-2).

Surface Temperature

Sixty-nine surface temperature measurements by 30 AWG "cement-on" chromel-alumel thermocouples will be made in different locations. These will include 13 measurements on the ceiling surface (Figure B-1), 20 on the four inside walls (Figure B-3), 3 on the floor and 22 will be kept for the surface temperature measurements at various locations on the "cabinets" (target). In addition, a total of 11 measurements will be made on the four outside walls and on the roof. These data will help determine the magnitude of wall and ceiling heat loss experienced during the tests.

Total Heat Flux Received by the Target Material

Twenty-seven "cement-on" heat flux sensors (Micro-foil Heat Flow Sensor, RdF No. 20452-3, RdF Corp., Hudson, NH) will be used on the ceiling and inside wall surfaces as well as on the target "cabinet" surfaces to measure the total heat flux received.

Gas-Species Concentration

Gas sampling ports are placed at several locations on the ceiling at vertical stations and at the exhaust ventilation. CO, CO₂, and O₂ concentrations will be multiplexed from 9 sampling ports (at the ceiling and vertical stations). CO₂ concentrations will be measured continuous at one ceiling location and in the exhaust duct. In addition, THC concentrations will be multiplexed from three ceiling sampling ports. Gas concentrations will be measured by 1) oxygen analyzers, Beckman Model 755 paramagnetic; 2) carbon dioxide analyzers, Beckman Model 864 infrared; 3) total hydrocarbon analyzers, Beckman Model 400 flame ionization; and 4) carbon monoxide analyzers, Beckman Model 864 infrared.

Gas Velocity

Gas velocities will be monitored at nine locations with bidirectional differential-pressure flow probes. These flow probes were developed at FMRC for large-scale fire tests^(B-3). These probes are able to sense and indicate flows in opposite directions with equal sensitivity and with relative insensitivity to the angle of the flow. Two flow probes will be combined in an assembly at each location and connected to electronic manometers in order to determine horizontal and vertical components of the gas velocity. The gas velocities measured with these flow probes will also be used to check velocity calculations from the sphere calorimeters.

Optical Density of Smoke

Optical density of "smoke" will be measured at three ceiling and three vertical locations by six smoke turbidimeters developed at FMRC^(B-4). One turbidimeter will be configured to measure optical density at three wavelengths which will enable particle size and number density of smoke to be calculated from the measurements. Additional details of the turbidimeter are given in Ref. B-4.

Smoke Detector

Three commercial smoke detectors (ionization or photoelectric) will be installed at the ceiling locations close to the smoke turbidimeters. Signals from these detectors will be monitored continuously to determine their response to smoke.

Mass Loss Rate

Mass loss rate will continuously be recorded for PMMA, heptane, and methanol fire sources, as well as for "cabinet materials" by means of a load cell system. The entire "cabinet", for example, will be placed on a platform positioned on top of the load cell system.

Pressure

Pressure differential (ΔP) will be measured at two locations within the test enclosure, two at the inlet and outlet ventilation, and two at the

OMIN2.RC

cabinet. ΔP will be measured with pressure transducers manufactured by Setra Systems (Model 261).

Fire Products Collector

The Fire Products Collector (FPC) at the 18.29-m test site of the Test Center will be used as the fire properties measuring apparatus in this program. A schematic of the FPC is presented in Figure B-4. The FPC is a large-capacity calorimeter which can measure fires in the megawatt range. It has a collecting funnel with a 6.10-m inlet diameter located at 7.93 m from the test floor. The FPC is connected to the pollution control system of the Test Center and can draw in, at its maximum capacity, $28 \text{ m}^3/\text{s}$ of cold flow. The apparatus, instrumented with thermocouples, velocity probes, and gas sampling probes, measures the velocity, temperature, and concentration of various gas species of the gas stream flowing through the system for calculation of the actual and convective heat release rates and generation rates of gaseous products such as CO_2 , CO , and total hydrocarbons as well as the oxygen depletion rate. Based on the oxygen depletion rate or generation of CO and CO_2 , the total heat release rate can also be calculated. Approximately 20 channels of computer data are associated with this FPC. A detailed description of the FPC can be found in Reference B-5.

REFERENCES - APPENDIX B

- B-1 Newman, J.S. and Croce, P.A., "A Simple Aspirated Thermocouple for Use in Fires," *Fire and Flammability*, Vol. II, October 1979.
- B-2 Newman, J.S. and Hill, J.P., "Assessment of Exposure Fire Hazards to Cable Trays," Factory Mutual Research Corporation, Report No. RC80-T-56, July 1980.
- B-3 McCaffray, B.J., and Heskestad, G., "A Robust Bidirectional Low-Velocity Probe for Flame and Fire Application," *Combustion and Flame*, pp. 125-127, 1976.
- B-4 Newman, J.S., "Fire Environments in Ventilated Rooms: Detection of Cable/Exposure Fires," Factory Mutual Research Corporation, FMRC J.I. OF0R3.RC, May 1982.
- B-5 Heskestad, G., "A Fire Products Collector for Calorimetry into the MW Range," Factory Mutual Research Corporation, Norwood, Massachusetts, FMRC J.I. OC2E1.RA, June 1981.

TABLE B-1
SANDIA FIRE TESTS CHANNEL MAP

| Channel No. | Description | Gain Code |
|-------------|-------------------------------------|-----------|
| 1 | Aspirated T/C, Sector 1, 0.98H | 3 |
| 2 | Aspirated T/C, Sector 1, 0.90H | 3 |
| 3 | Aspirated T/C, Sector 1, 0.70H | 3 |
| 4 | Aspirated T/C, Sector 1, 0.50H | 3 |
| 5 | Aspirated T/C, Sector 1, 0.30H | 3 |
| 6 | Aspirated T/C, Sector 2, 0.98H | 3 |
| 7 | Aspirated T/C, Sector 2, 0.90H | 3 |
| 8 | Aspirated T/C, Sector 2, 0.70H | 3 |
| 9 | Aspirated T/C, Sector 2, 0.50H | 3 |
| 10 | Aspirated T/C, Sector 2, 0.98H | 3 |
| 11 | Aspirated T/C, Sector 3, 0.98H | 3 |
| 12 | Aspirated T/C, Sector 3, 0.90H | 3 |
| 13 | Aspirated T/C, Sector 3, 0.70H | 3 |
| 14 | Aspirated T/C, Sector 3, 0.50H | 3 |
| 15 | Aspirated T/C, Sector 3, 0.30H | 3 |
| 16 | Aspirated T/C, Station 1, 0.98H | 3 |
| 17 | Aspirated T/C, Station 2, 0.98H | 3 |
| 18 | Aspirated T/C, Station 3, 0.98H | 3 |
| 19 | Aspirated T/C, Station 4, 0.98H | 3 |
| 20 | Aspirated T/C, Station 5, 0.98H | 3 |
| 21 | Aspirated T/C, Station 6, 0.98H | 3 |
| 22 | Aspirated T/C, Station 7, 0.98H | 3 |
| 23 | Aspirated T/C, Station 8, 0.98H | 3 |
| 24 | Aspirated T/C, Station 9, 0.98H | 3 |
| 25 | Aspirated T/C, Station 10, 0.98H | 3 |
| 26 | Aspirated T/C, Station 11, 0.98H | 3 |
| 27 | Aspirated T/C, Station 12, 0.98H | 3 |
| 28 | Aspirated T/C, Station 13, 0.98H | 3 |
| 29 | Aspirated T/C, Station 14, 0.98H | 3 |
| 30 | Aspirated T/C, Station 15, 0.98H | 3 |
| 31 | Aspirated T/C, Station 16, 0.98H | 3 |
| 32 | Bare bead gas T/C, Sector 1, 0.98H | 3 |
| 33 | Bare bead gas T/C, Sector 1, 0.70H | 3 |
| 34 | Bare bead gas T/C, Sector 1, 0.30H | 3 |
| 35 | Bare bead gas T/C, Sector 2, 0.98H | 3 |
| 36 | Bare bead gas T/C, Sector 2, 0.70H | 3 |
| 37 | Bare bead gas T/C, Sector 2, 0.30H | 3 |
| 38 | Bare bead gas T/C, Sector 3, 0.98H | 3 |
| 39 | Bare bead gas T/C, Sector 3, 0.70H | 3 |
| 40 | Bare bead gas T/C, Sector 3, 0.30H | 3 |
| 41 | Bare bead gas T/C, Station 1, 0.90H | 3 |
| 42 | Bare bead gas T/C, Station 1, 0.70H | 3 |
| 43 | Bare bead gas T/C, Station 1, 0.50H | 3 |
| 44 | Bare bead gas T/C, Station 1, 0.30H | 3 |
| 45 | Bare bead gas T/C, Station 2, 0.90H | 3 |
| 46 | Bare bead gas T/C, Station 2, 0.70H | 3 |
| 47 | Bare bead gas T/C, Station 2, 0.50H | 3 |
| 48 | Bare bead gas T/C, Station 2, 0.30H | 3 |
| 49 | Bare bead gas T/C, Station 3, 0.90H | 3 |
| 50 | Bare bead gas T/C, Station 3, 0.70H | 3 |

| | | |
|-----|---|---|
| 51 | Bare bead gas T/C, Station 3, 0.50H | 3 |
| 52 | Bare bead gas T/C, Station 3, 0.30H | 3 |
| 53 | Bare bead gas T/C, Station 4, 0.90H | 3 |
| 54 | Bare bead gas T/C, Station 4, 0.70H | 3 |
| 55 | Bare bead gas T/C, Station 4, 0.50H | 3 |
| 56 | Bare bead gas T/C, Station 4, 0.30H | 3 |
| 57 | Bare bead gas T/C, Station 5, 0.90H | 3 |
| 58 | Bare bead gas T/C, Station 5, 0.70H | 3 |
| 59 | Bare bead gas T/C, Station 5, 0.50H | 3 |
| 60 | Bare bead gas T/C, Station 5, 0.30H | 3 |
| 61 | Bare bead gas T/C, Station 6, 0.90H | 3 |
| 62 | Bare bead gas T/C, Station 6, 0.70H | 3 |
| 63 | Bare bead gas T/C, Station 6, 0.50H | 3 |
| 64 | Bare bead gas T/C, Station 6, 0.30H | 3 |
| 65 | Bare bead gas T/C, Station 7, 0.90H | 3 |
| 66 | Bare bead gas T/C, Station 7, 0.70H | 3 |
| 67 | Bare bead gas T/C, Station 7, 0.50H | 3 |
| 68 | Bare bead gas T/C, Station 7, 0.30H | 3 |
| 69 | Bare bead gas T/C, Station 8, 0.90H | 3 |
| 70 | Bare bead gas T/C, Station 8, 0.70H | 3 |
| 71 | Bare bead gas T/C, Station 8, 0.50H | 3 |
| 72 | Bare bead gas T/C, Station 8, 0.30H | 3 |
| 73 | Bare bead gas T/C, Station 9, 0.90H | 3 |
| 74 | Bare bead gas T/C, Station 9, 0.70H | 3 |
| 75 | Bare bead gas T/C, Station 9, 0.50H | 3 |
| 76 | Bare bead gas T/C, Station 9, 0.30H | 3 |
| 77 | Bare bead gas T/C, Station 10, 0.90H | 3 |
| 78 | Bare bead gas T/C, Station 10, 0.70H | 3 |
| 79 | Bare bead gas T/C, Station 10, 0.50H | 3 |
| 80 | Bare bead gas T/C, Station 10, 0.30H | 3 |
| 81 | Bare bead gas T/C, Station 17, 0.98H | 3 |
| 82 | Bare bead gas T/C, Station 17, 0.90H | 3 |
| 83 | Bare bead gas T/C, Station 17, 0.70H | 3 |
| 84 | Bare bead gas T/C, Station 17, 0.50H | 3 |
| 85 | Bare bead gas T/C, Station 17, 0.30H | 3 |
| 86 | Bare bead gas T/C, Station 18, 0.98H | 3 |
| 87 | Bare bead gas T/C, Station 18, 0.90H | 3 |
| 88 | Bare bead gas T/C, Station 18, 0.70H | 3 |
| 89 | Bare bead gas T/C, Station 18, 0.50H | 3 |
| 90 | Bare bead gas T/C, Station 18, 0.30H | 3 |
| 91 | Bare bead gas T/C, Ventilation inlet | 3 |
| 92 | Bare bead gas T/C, Ventilation outlet | 3 |
| 93 | Inner ceiling surface T/C, Sector 1 | 3 |
| 94 | Outer ceiling surface T/C, Sector 1 | 3 |
| 95 | Inner ceiling surface T/C, Sector 2 | 3 |
| 96 | Outer ceiling surface T/C, Sector 2 | 3 |
| 97 | Inner ceiling surface T/C, Sector 3 | 3 |
| 98 | Outer ceiling surface T/C, Sector 3 | 3 |
| 99 | Inner ceiling surface T/C, Station 1 | 3 |
| 100 | Inner ceiling surface T/C, Station 2 | 3 |
| 101 | Inner ceiling surface T/C, Station 3 | 3 |
| 102 | Inner ceiling surface T/C, Station 4 | 3 |
| 103 | Inner ceiling surface T/C, Station 5 | 3 |
| 104 | Inner ceiling surface T/C, Station 6 | 3 |
| 105 | Inner ceiling surface T/C, Station 7 | 3 |
| 106 | Inner ceiling surface T/C, Station 8 | 3 |
| 107 | Inner ceiling surface T/C, Station 9 | 3 |
| 108 | Inner ceiling surface T/C, Station 10 | 3 |
| 109 | Inner wall surface T/C, North center, 0.90H | 3 |

| | | |
|-----|---|---|
| 110 | Outer wall surface T/C, North center, 0.90H | 3 |
| 111 | Inner wall surface T/C, North center, 0.50H | 3 |
| 112 | Outer wall surface T/C, North center, 0.90H | 3 |
| 113 | Inner wall surface T/C, North right, 0.90H | 3 |
| 114 | Inner wall surface T/C, North right, 0.50H | 3 |
| 115 | Inner wall surface T/C, North left, 0.90H | 3 |
| 116 | Inner wall surface T/C, North left, 0.50H | 3 |
| 117 | Inner wall surface T/C, South center, 0.90H | 3 |
| 118 | Outer wall surface T/C, South center, 0.90H | 3 |
| 119 | Inner wall surface T/C, South center, 0.90H | 3 |
| 120 | Outer wall surface T/C, South center, 0.90H | 3 |
| 121 | Inner wall surface T/C, South right, 0.90H | 3 |
| 122 | Inner wall surface T/C, South right, 0.50H | 3 |
| 123 | Inner wall surface T/C, South left, 0.90H | 3 |
| 124 | Inner wall surface T/C, South left, 0.50H | 3 |
| 125 | Inner wall surface T/C, East right, 0.90H | 3 |
| 126 | Outer wall surface T/C, East right, 0.90H | 3 |
| 127 | Inner wall surface T/C, East right, 0.50H | 3 |
| 128 | Inner wall surface T/C, East left, 0.90H | 3 |
| 129 | Outer wall surface T/C, East left, 0.90H | 3 |
| 130 | Inner wall surface T/C, East left, 0.50H | 3 |
| 131 | Inner wall surface T/C, West right, 0.90H | 3 |
| 132 | Outer wall surface T/C, West right, 0.90H | 3 |
| 133 | Inner wall surface T/C, West right, 0.50H | 3 |
| 134 | Inner wall surface T/C, West left, 0.90H | 3 |
| 135 | Outer wall surface T/C, West left, 0.90H | 3 |
| 136 | Inner wall surface T/C, West left, 0.50H | 3 |
| 137 | Floor surface T/C, Sector 1 | 3 |
| 138 | Floor surface T/C, Sector 2 | 3 |
| 139 | Floor surface T/C, Sector 3 | 3 |
| 140 | Cabinet surface T/C #1 | 3 |
| 141 | Cabinet surface T/C #2 | 3 |
| 142 | Cabinet surface T/C #3 | 3 |
| 143 | Cabinet surface T/C #4 | 3 |
| 144 | Cabinet surface T/C #5 | 3 |
| 145 | Cabinet surface T/C #6 | 3 |
| 146 | Cabinet surface T/C #7 | 3 |
| 147 | Cabinet surface T/C #8 | 3 |
| 148 | Cabinet surface T/C #9 | 3 |
| 149 | Cabinet surface T/C #10 | 3 |
| 150 | Cabinet surface T/C #11 | 3 |
| 151 | Cabinet surface T/C #12 | 3 |
| 152 | Cabinet surface T/C #13 | 3 |
| 153 | Cabinet surface T/C #14 | 3 |
| 154 | Cabinet surface T/C #15 | 3 |
| 155 | Cabinet surface T/C #16 | 3 |
| 156 | Cabinet surface T/C #17 | 3 |
| 157 | Cabinet surface T/C #18 | 3 |
| 158 | Cabinet surface T/C #19 | 3 |
| 159 | Cabinet surface T/C #20 | 3 |
| 160 | Cabinet surface T/C #21 | 3 |
| 161 | Cabinet surface T/C #22 | 3 |
| 162 | Large sphere calorimeter, Sector 1, 0.98H | 3 |
| 163 | Small sphere calorimeter, Sector 1, 0.98H | 3 |
| 164 | Large sphere calorimeter, Sector 1, 0.70H | 3 |
| 165 | Small sphere calorimeter, Sector 1, 0.70H | 3 |
| 166 | Large sphere calorimeter, Sector 1, 0.30H | 3 |
| 167 | Small sphere calorimeter, Sector 1, 0.30H | 3 |
| 168 | Large sphere calorimeter, Sector 2, 0.98H | 3 |

| | | |
|-----|---|---|
| 169 | Small sphere calorimeter, Sector 2, 0.98H | 3 |
| 170 | Large sphere calorimeter, Sector 2, 0.70H | 3 |
| 171 | Small sphere calorimeter, Sector 2, 0.70H | 3 |
| 172 | Large sphere calorimeter, Sector 2, 0.30H | 3 |
| 173 | Small sphere calorimeter, Sector 2, 0.30H | 3 |
| 174 | Large sphere calorimeter, Sector 3, 0.98H | 3 |
| 175 | Small sphere calorimeter, Sector 3, 0.98H | 3 |
| 176 | Large sphere calorimeter, Sector 3, 0.70H | 3 |
| 177 | Small sphere calorimeter, Sector 3, 0.70H | 3 |
| 178 | Large sphere calorimeter, Sector 3, 0.30H | 3 |
| 179 | Small sphere calorimeter, Sector 3, 0.30H | 3 |
| 180 | Horizontal flow probe, Sector 1, 0.98H | 8 |
| 181 | Vertical flow probe, Sector 1, 0.98H | 8 |
| 182 | Horizontal flow probe, Sector 1, 0.70H | 8 |
| 183 | Vertical flow probe, Sector 1, 0.70H | 8 |
| 184 | Horizontal flow probe, Sector 1, 0.30H | 8 |
| 185 | Vertical flow probe, Sector 1, 0.30H | 8 |
| 186 | Horizontal flow probe, Sector 2, 0.98H | 8 |
| 187 | Vertical flow probe, Sector 2, 0.98H | 8 |
| 188 | Horizontal flow probe, Sector 2, 0.70H | 8 |
| 189 | Vertical flow probe, Sector 2, 0.70H | 8 |
| 190 | Horizontal flow probe, Sector 2, 0.30H | 8 |
| 191 | Vertical flow probe, Sector 2, 0.30H | 8 |
| 192 | Horizontal flow probe, Sector 3, 0.98H | 8 |
| 193 | Vertical flow probe, Sector 3, 0.98H | 8 |
| 194 | Horizontal flow probe, Sector 3, 0.70H | 8 |
| 195 | Vertical flow probe, Sector 3, 0.70H | 8 |
| 196 | Horizontal flow probe, Sector 3, 0.30H | 8 |
| 197 | Vertical flow probe, Sector 3, 0.30H | 8 |
| 198 | Pressure differential, Ventilation inlet | 8 |
| 199 | Pressure differential, Ventilation outlet | 8 |
| 200 | Pressure differential, Enclosure | 8 |
| 201 | Pressure differential, Atmosphere | 8 |
| 202 | Pressure differential, Cabinet inlet | 8 |
| 203 | Pressure differential, Cabinet outlet | 8 |
| 204 | CO2 analyzer(multiplexed), Sectors 1-3, 0.98H | 8 |
| 205 | CO analyzer(multiplexed), Sectors 1-3, 0.98H | 8 |
| 206 | O2 analyzer(multiplexed), Sectors 1-3, 0.98H | 8 |
| 207 | THC analyzer(multiplexed), Sectors 1-3, 0.98H | 8 |
| 208 | CO2 analyzer(multiplexed), Sectors 1-3, 0.70H | 8 |
| 209 | CO analyzer(multiplexed), Sectors 1-3, 0.70H | 8 |
| 210 | CO2 analyzer(multiplexed), Sectors 1-3, 0.30H | 8 |
| 211 | CO analyzer(multiplexed), Sectors 1-3, 0.30H | 8 |
| 212 | CO2 analyzer, Sector 2, 0.98H | 8 |
| 213 | CO2 analyzer, Ventilation outlet | 8 |
| 214 | Blue optical density, Sector 1, 0.98H | 7 |
| 215 | Blue optical density, Sector 1, 0.30H | 7 |
| 216 | Blue optical density, Sector 2, 0.98H | 7 |
| 217 | Red optical density, Sector 2, 0.98H | 7 |
| 218 | IR optical density, Sector 2, 0.98H | 7 |
| 219 | Blue optical density, Sector 2, 0.30H | 7 |
| 220 | Blue optical density, Sector 3, 0.98H | 7 |
| 221 | Blue optical density, Sector 3, 0.30H | 7 |
| 222 | Ceiling heat flux, Sector 1 | 2 |
| 223 | Ceiling heat flux, Sector 2 | 2 |
| 224 | Ceiling heat flux, Sector 3 | 2 |
| 225 | Ceiling heat flux, Station 1 | 2 |
| 226 | Ceiling heat flux, Station 2 | 2 |
| 227 | Ceiling heat flux, Station 3 | 2 |

| | | |
|-----|-------------------------------------|---|
| 228 | Ceiling heat flux, Station 8 | 2 |
| 229 | Ceiling heat flux, Station 9 | 2 |
| 230 | Ceiling heat flux, Station 10 | 2 |
| 231 | Wall heat flux, North center, 0.90H | 2 |
| 232 | Wall heat flux, North right, 0.90H | 2 |
| 233 | Wall heat flux, North left, 0.90H | 2 |
| 234 | Wall heat flux, South center, 0.90H | 2 |
| 235 | Wall heat flux, South right, 0.90H | 2 |
| 236 | Wall heat flux, South left, 0.90H | 2 |
| 237 | Wall heat flux, East right, 0.90H | 2 |
| 238 | Wall heat flux, East left, 0.90H | 2 |
| 239 | Wall heat flux, West right, 0.90H | 2 |
| 240 | Wall heat flux, West left, 0.90H | 2 |
| 241 | Floor heat flux, Sector 1 | 2 |
| 242 | Floor heat flux, Sector 2 | 2 |
| 243 | Floor heat flux, Sector 3 | 2 |
| 244 | Cabinet heat flux #1 | 2 |
| 245 | Cabinet heat flux #2 | 2 |
| 246 | Cabinet heat flux #3 | 2 |
| 247 | Cabinet heat flux #4 | 2 |
| 248 | Cabinet heat flux #5 | 2 |
| 249 | Mass loss | - |

× Inner Surface T/C

○ Inner Surface Heat Flux

□ Outer Surface T/C

▣ Ventilation Inlet Port
(1.5'x1.5')

B-10

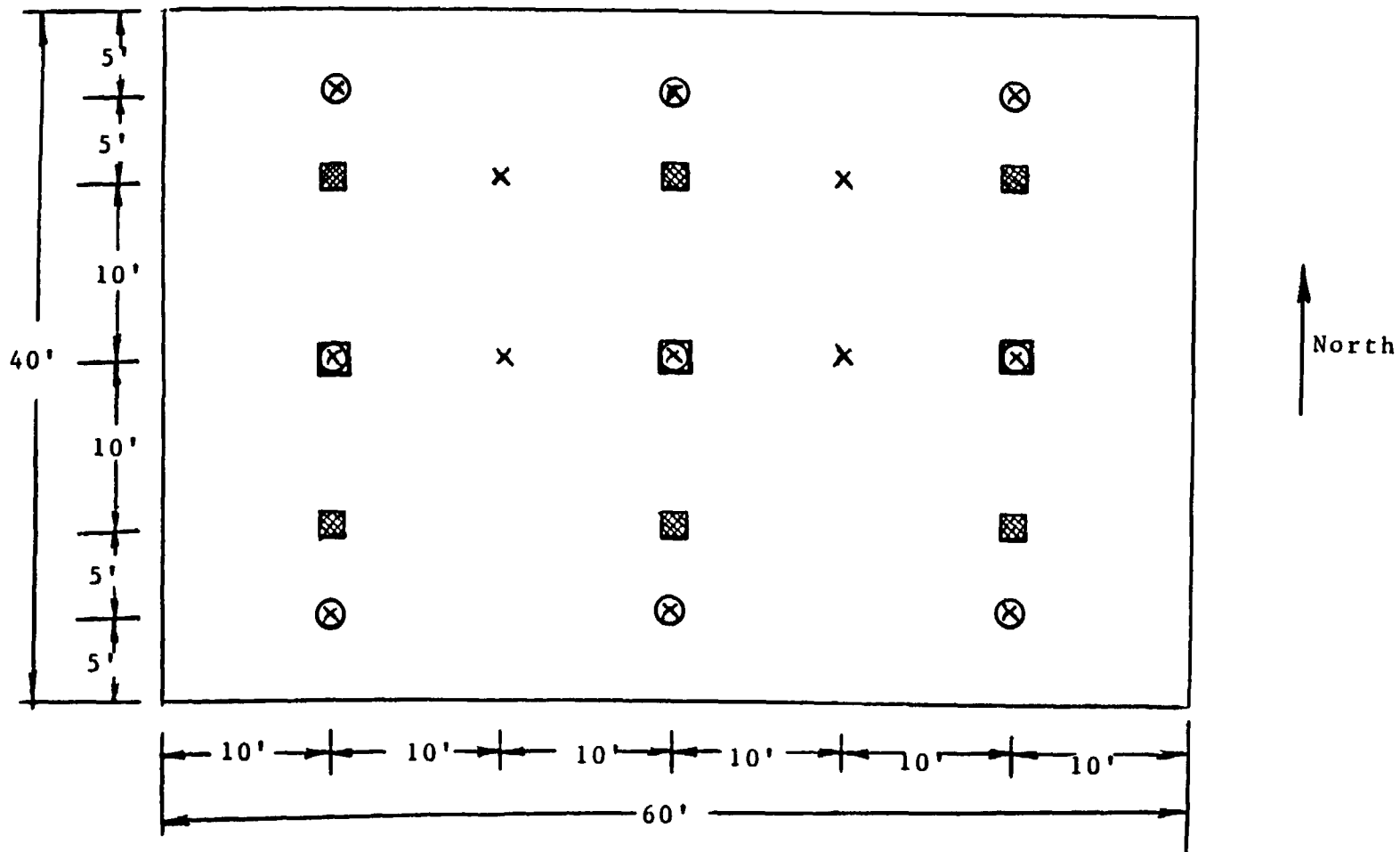


FIGURE B-1 INSTRUMENTATION LAYOUT - CEILING (View looking into enclosure)

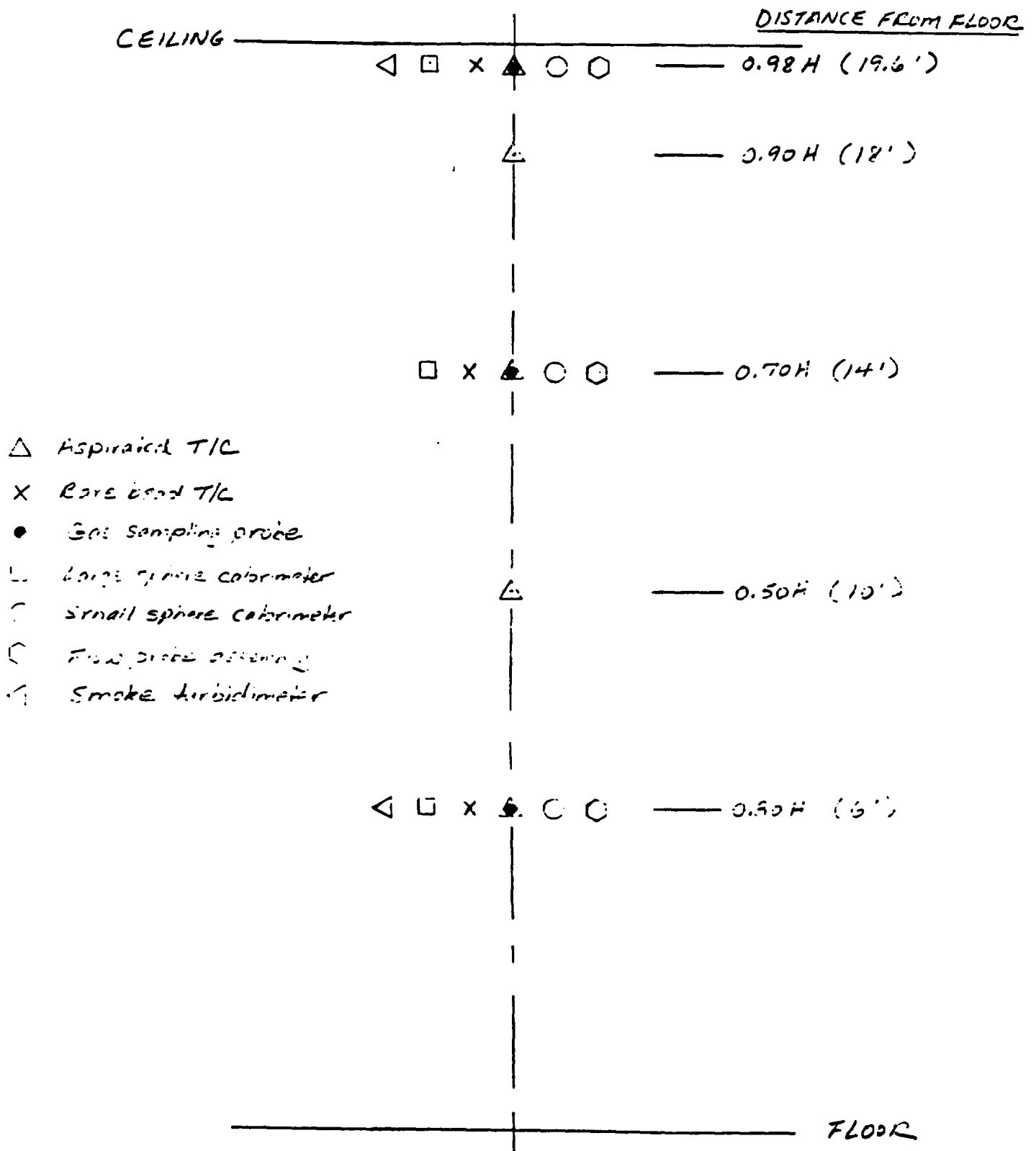


FIGURE B-2 INSTRUMENTATION LAYOUT - SECTOR CONFIGURATION

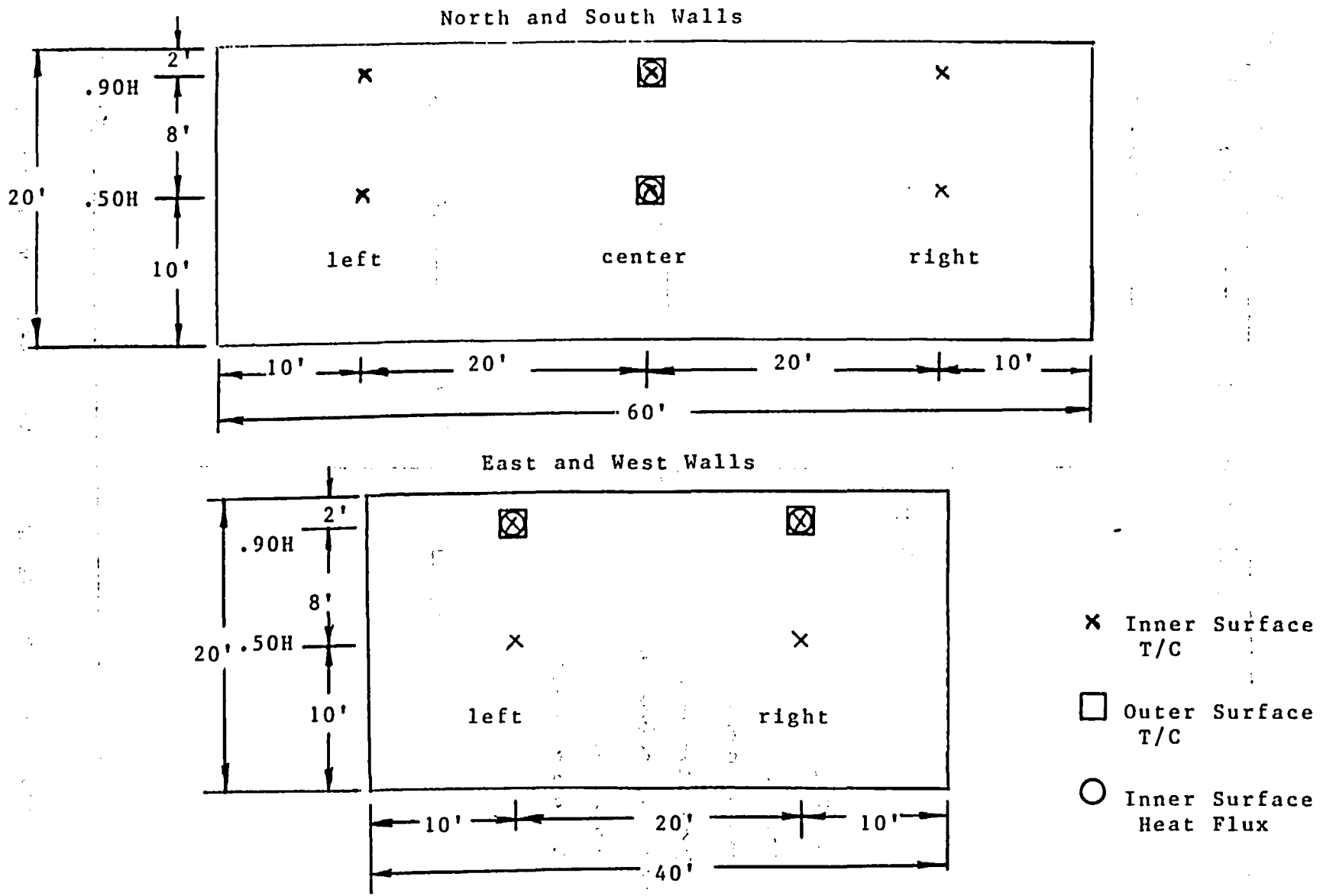
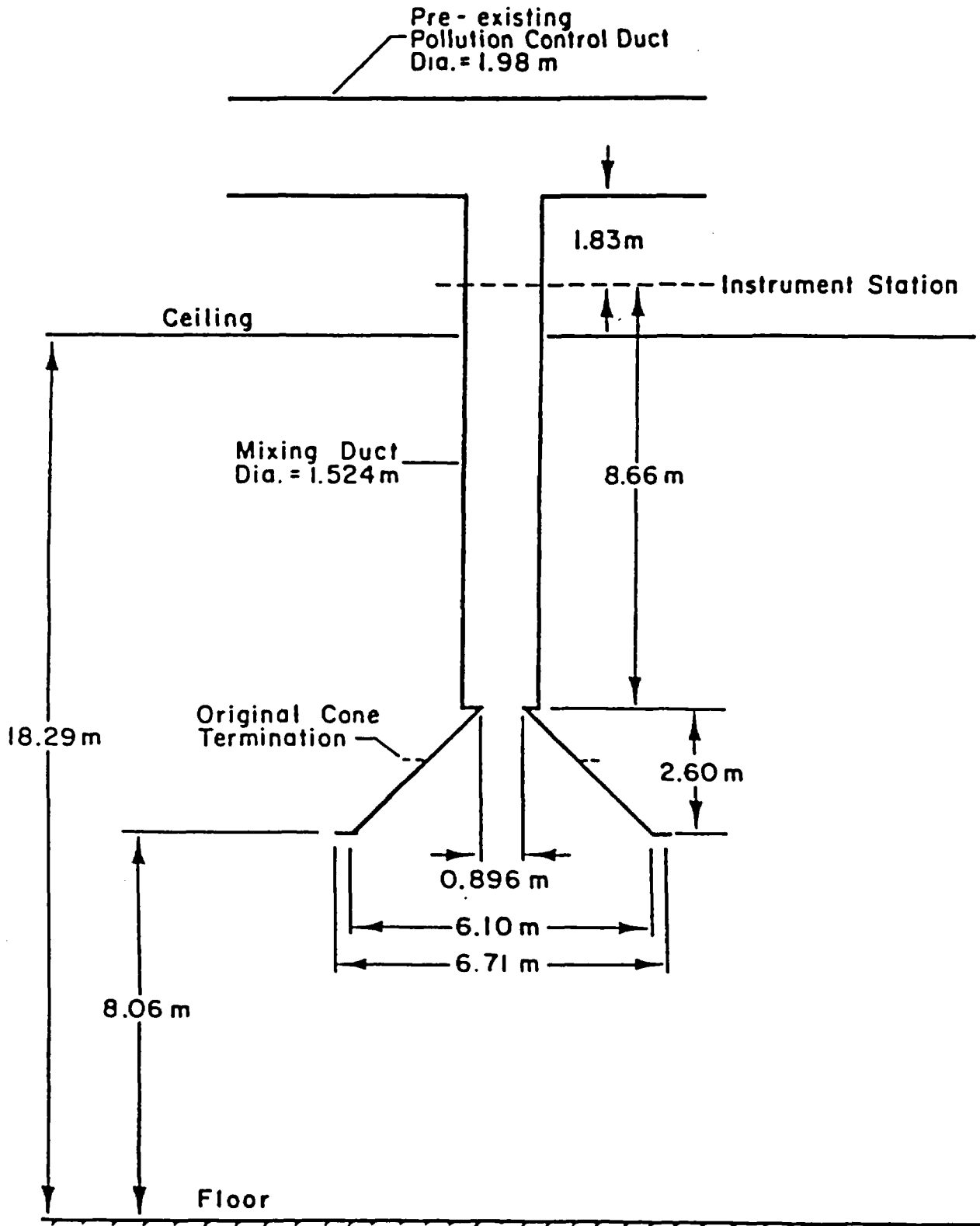


FIGURE B-3 INSTRUMENTATION LAYOUT - WALLS (Left/right relative to view looking into enclosure)



a) Flow Boundaries

FIGURE B-4 FIRE PRODUCTS COLLECTOR



Appendix C

Calculation of Heat Release Rate

Because of certain unique aspects of this test program, special consideration is required in the calculation of heat release rates for the test fires. The heat release rate of a fire can be estimated based on the generation rate of carbon dioxide. This is expressed as:

$$(\text{HRR}) = K_1 \dot{g}_{\text{CO}_2} \quad (1).$$

Here (HRR) stands for heat release rate, (\dot{g}_{CO_2}) is the mass generation rate of carbon dioxide, and (K_1) is a constant that quantifies the heat released by the fuel of concern per unit mass of carbon dioxide generated. Note that the constant (K_1) is a function of the fuel material. Corrections to this estimation for the generation of carbon monoxide caused by incomplete combustion can be made; however, for the present discussion the relationship described in Equation 1 will be used.

In most simple test cases the generation rate of carbon dioxide is estimated based only on the outflow rate of carbon dioxide. This implies an assumption that accumulation of carbon dioxide within the test enclosure or test structure can be neglected. In most test situations in which the test enclosure is relatively small and configured such that fire products are efficiently drawn off for analysis, this assumption is valid. In the present case, this assumption would not be valid. Because of the large size of the test enclosure (48000 ft³ or 1360 m³), a significant amount of the fire generated products of combustion accumulate within the test enclosure. Thus, in order to estimate the test fire heat release rates based on carbon dioxide generation calorimetry, one must account for accumulation of carbon dioxide within the test enclosure.

Consider the enclosure used for these tests. The generation of CO₂ can be expressed as the sum of the net outflow and the net accumulation rates of CO₂:

$$\dot{g}_{\text{CO}_2}(t) = \dot{F}_{\text{CO}_2}(t) + \dot{A}_{\text{CO}_2}(t) \quad (2).$$

Each term is a function of time (the time functionality (t) will be dropped for convenience). The flow rate is expressed as the difference between the outflow and inflow rates for CO₂:

$$\dot{F}_{CO_2} = (\dot{m}_{CO_2})_{out} - (\dot{m}_{CO_2})_{in} \quad (3).$$

where the mass flow rate of CO_2 (\dot{m}_{CO_2}) can be expressed in terms of the total volume flow rate (\dot{V}), the volumetric CO_2 concentration (C), and the density of CO_2 (ρ) as:

$$\dot{F}_{CO_2} = (\dot{V}\rho C)_{out} - (\dot{V}\rho C)_{in} \quad (4).$$

This expression can be further simplified by assuming that the inlet and outlet total volume flow rates are equal and by using the ideal gas law to substitute for CO_2 density:

$$\dot{F}_{CO_2} = \dot{V} \left[\left\{ \frac{P}{TR} C \right\}_{out} - \left\{ \frac{P}{TR} C \right\}_{in} \right] \quad (5).$$

where P is absolute pressure, T is absolute temperature, and R is the gas constant for CO_2 . If pressure is assumed to be constant (a good assumption as absolute pressure is used) then:

$$\dot{F}_{CO_2} = \frac{P}{R} \dot{V} \left[\left\{ \frac{C}{T} \right\}_{out} - \left\{ \frac{C}{T} \right\}_{in} \right] \quad (6).$$

The accumulation term in Equation (2) can be expressed as an integral over the enclosure volume of the mass accumulation rate:

$$\dot{A}_{CO_2} = \frac{d}{dt} \left[\int_{V_e} m'_{CO_2} dv \right] \quad (7).$$

where (m') is the mass per unit volume. Using density and volumetric concentration this can be expressed as:

$$\dot{A}_{CO_2} = \frac{d}{dt} \left[\int_{V_e} \rho C dv \right] \quad (8).$$

and again using the ideal gas law to substitute for the density of CO₂:

$$\dot{A}_{CO_2} = \frac{d}{dt} \left[\int_{V_e} \frac{P}{RT} C \, dV \right] \quad (9).$$

and assuming constant pressure:

$$\dot{A}_{CO_2} = \frac{P}{R} \frac{d}{dt} \left[\int_{V_e} \frac{C}{T} \, dV \right] \quad (10).$$

It is this integral that must be approximated in order to evaluate Equation (2). One method that has met with relative success is to assume that all of the CO₂ accumulation occurs in the developing hot layer, and that the developing hot layer can be lumped into three discrete layers. The first layer (HL1) is assumed to extend from the ceiling (20') to the level of the inlet ports (16'). The second layer (HL2) is assumed to extend from (16') to the level of the lowest instrumentation plane (6'). The final layer (HL3) extends from (6') to the floor. Each of these layers is assumed to be well mixed. The concentration of CO₂ and gas temperature for each of these three layer is assumed to be characterized by the sector 2 instrumentation at .98H, .7H, and .3H respectively. Thus the integral expressed in Equation (10) can be expressed:

$$\dot{A}_{CO_2} = \frac{A_e P}{R} \frac{d}{dt} \left[\left\{ \frac{DC}{T} \right\}_{HL1} + \left\{ \frac{DC}{T} \right\}_{HL2} + \left\{ \frac{DC}{T} \right\}_{HL3} \right] \quad (11).$$

where A_e is the floor area of the enclosure (2400 ft² or 223 m²), and D represents the depth of each layer. The derivative terms can be evaluated as follows:

$$\frac{d}{dt} \left\{ \frac{DC}{T} \right\} = \frac{D}{T} \frac{dC}{dt} + \frac{DC}{T^2} \frac{dT}{dt} + \frac{C}{T} \frac{dD}{dt} \quad (12).$$

During initial attempts to calculate heat release rates using this method and the raw data, it was found that minor fluctuations in the carbon dioxide measurements resulted in very large

fluctuations in calculated heat release rates because of the heavy weighting of the derivative terms. Consequently a series of second order quadratic curves was fit to the raw data and the resulting curve fit values used in the calculation process. As the CO₂ measurements tend to be well behaved and change rather smoothly, these curve fits match the raw data quite well as shown by Figure C-1.

The calculated heat release rate for Test 4 is shown in Figure C-2. This compares quite well with the expected profile, especially as contrasted by the values based only on the outflow rate. The values shown were based on an assumption that the depth of each hot layer was constant at 4, 10, and 6 feet respectively. This results in some simplification of Equation 12 as the final term then goes to zero. Time derivative terms are estimated based on a central difference approximation.

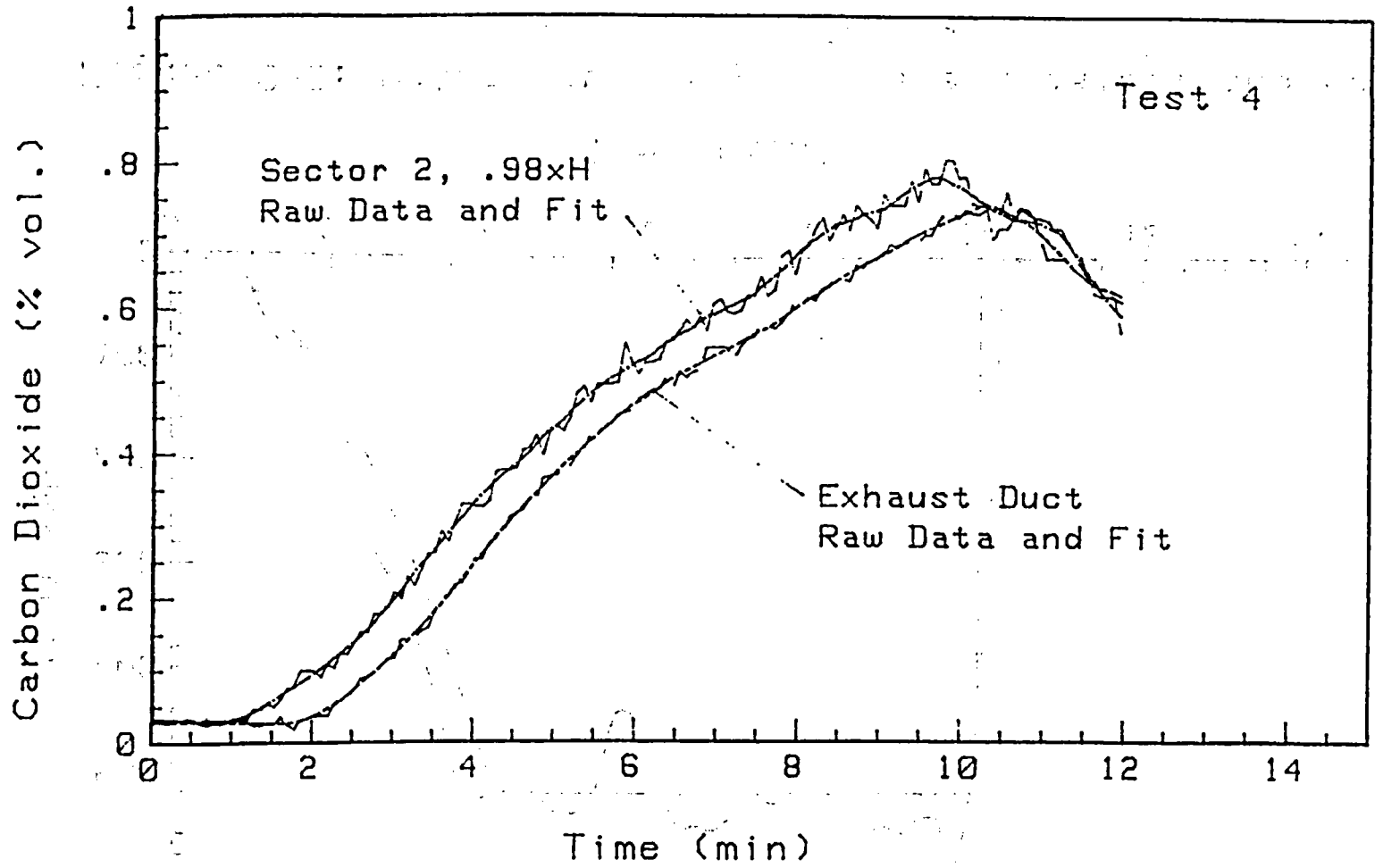


Figure C-1: Carbon dioxide data and curve fits used in calculation of heat release rate.

C-6

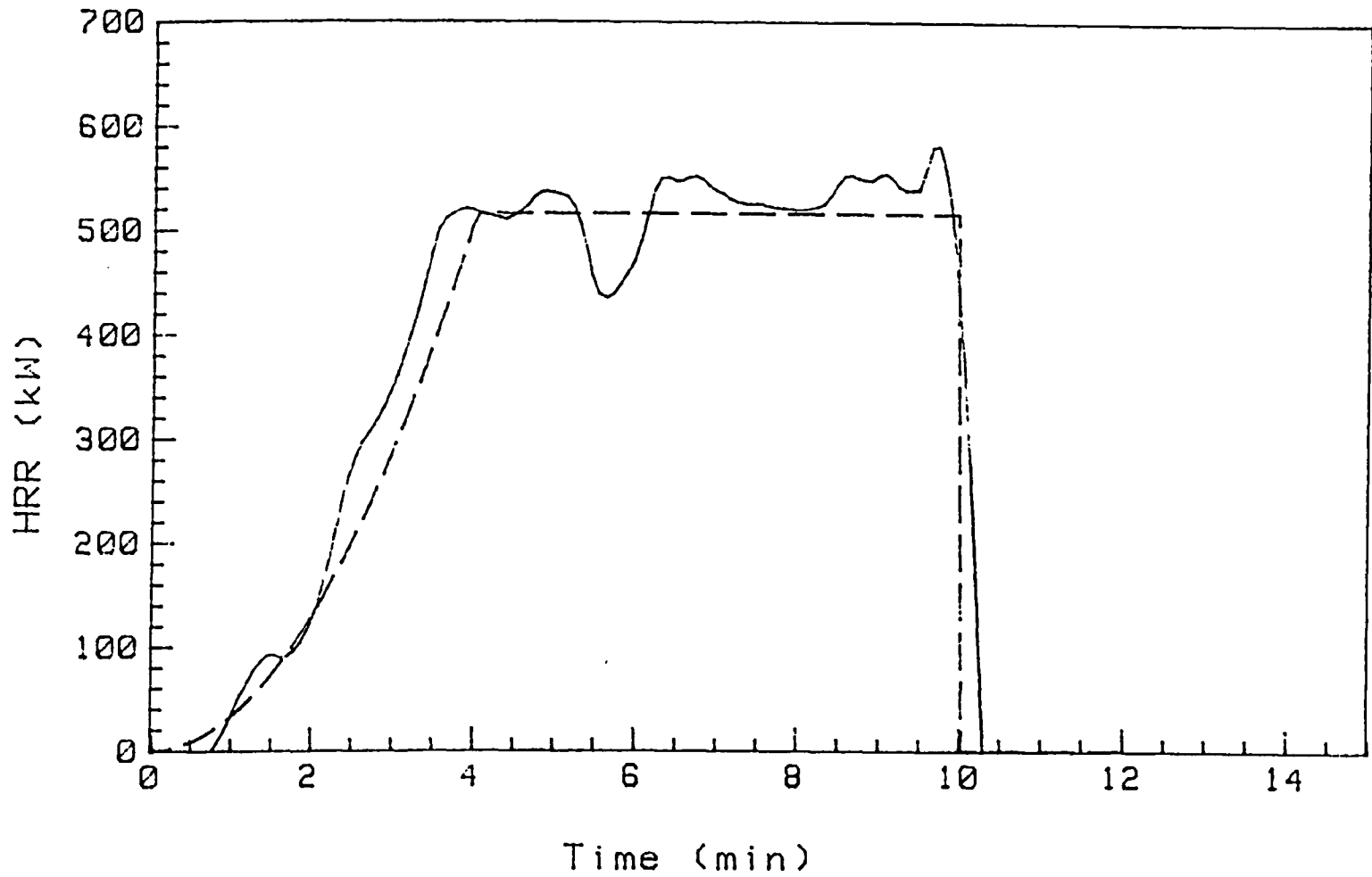


Figure C-2: Actual burner profile and calculated heat release rate for Test 4.

Nomenclature

- \dot{g}_{CO_2} - mass generation rate of CO_2
- K_1 - heat generation per mass CO_2 generated
- \dot{A} - mass accumulation rate of CO_2
- A_e - enclosure floor area (223 m²)
- \dot{F}_{CO_2} - net mass flow rate of CO_2 out of enclosure
- \dot{m}_{CO_2} - mass flow rate of CO_2
- m'_{CO_2} - mass of CO_2 per unit volume
- \dot{V} - volume flow rate
- ρ - density of CO_2
- C - volumetric concentration of CO_2
- T - absolute temperature
- t - time
- P - absolute pressure
- R - gas constant for CO_2
- D - depth of hot layer
- $\frac{d}{dt}$ - derivative with respect to time

DISTRIBUTION:

U.S. Government Printing Office
Receiving Branch (Attn: NRC Stock)
8610 Cherry Lane
Laurel, MD 20707
(200 copies for RP)

U.S. Nuclear Regulatory Commission
Electrical Engineering Branch
Attn: A. Datta (5)
Mail Stop NL 5650
Washington, DC 20555

Impell Corporation
Attn: Collin A. Lewis
350 Lennon Lane
Walnut Creek, CA 94598

Professional Loss Control, Inc.
Attn: Kenneth Dungan
P.O. Box 446
Oak Ridge, TN 37830

Electric Power Research Institute
Nuclear Power Division
Attn: Joseph Matte III
3412 Hillview Avenue
Palo Alto, CA 94304

Risk Management
Tennessee Valley Authority
Attn: Ralph Thompson
5N 79A Lookout Place
Chattanooga, TN 37402-2801

ANI
Exchange Building, Suite 245
Attn: Dotti Sherman, Library
270 Farmington Avenue
Farmington, CT 06032

Underwriters Laboratories
Attn: Leon Przybyla
333 Pfingston Road
Northbrook, IL 60062

M&M Protection Consultants
Attn: Stan Chingo
222 South Riverside Plaza
Chicago, IL 60606

Impell Corporation
Attn: John E. Echternacht
350 Lennon Lane
Walnut Creek, CA 94598

Lawrence Livermore Laboratory
Attn: Harry K. Hasegawa
P.O. Box 5505 L-442
Livermore, CA 94550

Clinch River Breeder Reactor Plant
CRBRP Project
Attn: Larry W. Clark
P.O. Box U
Oak Ridge, TN 37830

Patton Fire Suppression Systems, Inc.
Attn: Richard Patton
4740 Myrtle Avenue, Suite B
Sacramento, CA 95841

Electricite De France
Thermal Production Headquarters
Attn: Jean-Pierre Berthet
EDF-DSRE-6, Rue Ampere
BP 114
93203 Saint Denis Cedex 1
FRANCE

Factory Mutual Research Corporation
Attn: Jeff Newman
1151 Boston-Providence Hwy.
Norwood, MA 02062

Florida Power Corporation
Attn: L. R. Perkins
System Fire Protection Coordinator
6115 Park Blvd.
Pinellas Park, FL 33565

American Electric Power Service Co.
Attn: Jack D. Grier
Fire Protection and HVAC Section
1 Riverside Plaza
P.O. Box 16631
Columbus, OH 43216-6631

Commonwealth Edison
Attn: Tom Grey
72 W. Adams Street
Room 1248
Chicago, IL 60603

Grinnell Fire Protection Co.
Attn: Joe Priest
10 Dorrance Street
Providence, RI 02903

Brookhaven National Laboratories
Attn: John Boccio
Bldg. 130
Upton, NY 11793

U.S. Department of Energy
Albuquerque Operations Office
Attn: Andrew J. Pryor
P.O. Box 5400
Albuquerque, NM 87115

Edison Electric Institute
Attn: Jim Evans
1111 19th Street, NW
Washington, DC 20036-3691

Dr. Ulrich Heinz Schneider
Gesamthochschule Kassel
Universitat des Landes Hessen
FB 14, Postfach 101380
3500 Kassel, FRG

Dr. Dietmar Hosser
Koning und Heunisch
Letzter Hasenpfach 21
6000 Frankfurt/Main 70,
FRG

NUPEC
No. 2 Akiyama Building
Attn: Kenji Takumi
6-2, 3-Chome, Toranomon
Minatoku, Tokyo 105,
JAPAN

Mr. Liemersdorf
Gesellschaft fur Reaktorsicherheit
Schwertnergasse 1
D-5000 Koln 1,
FRG

Centre Scientifique et
Technique du Batiment
Station de Recherche
Attn: Xavier Bodart
84 Avenue Jean-Jaures-
Champs-sur-Marne
77428 Marne-La-Vallee Cedex 2
FRANCE

Societe Bertin & Cie
BP No. 3
Attn: Serge Galant
78373 Plaisir Cedex
FRANCE

M. Allen Matteson, Jr.
Code 1740.2
Ship Protection Division
Department of the Navy
David W. Taylor Naval Ship
Research and Development Center
Headquarters
Bethesda, MD 20084-5000

Mr. David Satterfield
National Center #4, Room 311
Naval Sea System Command (56Y52)
Washington, DC 20362

U.S. Department of Energy (2)
Attn: Carl A. Caves
Walter W. Maybee
Mail Stop EH-34
Washington, DC 20545

U.S. Department of Energy
Attn: Justin T. Zamirowski
9800 S. Cass Avenue
Argonne, IL 60439

3141 S. A. Landenberger (5)
3151 W. L. Garner
6400 D. J. McCloskey
6410 N. R. Ortiz
6417 D. D. Carlson
6420 J. V. Walker
6440 D. A. Dahlgren
6442 W. A. von Riesemann
6447 M. J. Jacobus
6447 D. King
6447 V. Nicolette
6447 S. P. Nowlen (25)
6448 D. L. Berry
6448 B. L. Spletzer
6448 W. T. Wheelis
8024 P. W. Dean

| | | | |
|---|--|---|--|
| NRC FORM 335 (2-84) NRCM 1102, 3201, 3202 BIBLIOGRAPHIC DATA SHEET SEE INSTRUCTIONS ON THE REVERSE | | U.S. NUCLEAR REGULATORY COMMISSION 1 REPORT NUMBER (Assigned by TIDC, add Vol. No., if any) NUREG/CR-4681 SAND86-1296 | |
| 2. TITLE AND SUBTITLE Enclosure Environment Characterization Testing For The Base Line Validation of Computer Fire Simulation Codes | | 3 LEAVE BLANK | |
| 5. AUTHOR(S) S. P. Nowlen | | 4 DATE REPORT COMPLETED MONTH YEAR March 1987 | |
| 7. PERFORMING ORGANIZATION NAME AND MAILING ADDRESS (Include Zip Code) Sandia National Laboratories Albuquerque, NM 87185 | | 6 DATE REPORT ISSUED MONTH YEAR March 1987 | |
| 10 SPONSORING ORGANIZATION NAME AND MAILING ADDRESS (Include Zip Code) U. S. Nuclear Regulatory Commission Electrical Engineering Branch Washington, D.C. 20555 | | 8 PROJECT-TASK-WORK UNIT NUMBER 9 FUND OR GRANT NUMBER A-1010 | |
| 12 SUPPLEMENTARY NOTES | | 11a TYPE OF REPORT b PERIOD COVERED (Inclusive Dates) | |
| 13 ABSTRACT (200 words or less) This report describes a series of fire tests conducted under the direction of Sandia National Laboratories for the U. S. Nuclear Regulatory Commission. The primary purpose of these tests was to provide data against which to validate computer fire environment simulation models to be used in the analysis of nuclear power plant enclosure fire situations. Examples of the data gathered during three of the tests are presented, though the primary objective of this report is to provide a timely description of the test effort itself. These tests were conducted in an enclosure measuring 60x40x20 feet. All of the tests utilized forced ventilation conditions typical of nuclear power plant installations. A total of 22 tests using simple gas burner, heptane pool, methanol pool, and PMMA solid fires was conducted. Four of these tests were conducted with a full-scale control room mockup in place. Parameters varied during testing were fire intensity, enclosure ventilation rate, and fire location. Data gathered included air temperatures, air velocities, radiative and convective heat flux levels, optical smoke densities, inner and outer enclosure surface temperatures, enclosure surface heat flux levels, and gas concentrations within the enclosure in the exhaust stream. | | | |
| 14 DOCUMENT ANALYSIS -- KEYWORDS/DESCRIPTORS Fire Testing Fire Characterization Fire Modeling d. IDENTIFIERS/OPEN-ENDED TERMS Enclosure Fire Testing Computer Fire Simulation Validation Testing Nuclear Power Plants | | 15 AVAILABILITY STATEMENT Unlimited 16 SECURITY CLASSIFICATION (This paper) Unclassified (This report) Unclassified 17 NUMBER OF PAGES 18 PRICE | |

P. MADDEN

BD-1